An extension of the Czjzek model for the distributions of electric field gradients in disordered solids and an application to NMR spectra of ^{71}Ga in chalcogenide glasses

2010 J. Phys.: Condens. Matter 22 065402

(http://iopscience.iop.org/0953-8984/22/6/065402)

J. Phys.: Condens. Matter **22** (2010) 065402 (17pp) doi:10.1088/0953-8984/22/6/065402

An extension of the Czjzek model for the distributions of electric field gradients in disordered solids and an application to NMR spectra of ^{71}Ga in chalcogenide glasses

Gérard Le Caër[1,4], Bruno Bureau[2] and Dominique Massiot[3]

[1] Institut de Physique de Rennes, UMR UR1-CNRS 6251, Université de Rennes I, Campus de Beaulieu, Bâtiment 11A, 35042 Rennes Cedex, France
[2] Equipe Verres et Céramiques, UMR-CNRS 6226 Sciences Chimiques de Rennes, Université de Rennes 1, Campus de Beaulieu, 35042 Rennes Cedex, France
[3] Centre de Recherches sur les Matériaux à Hautes Températures, UPR 4212 CNRS, 1D avenue de la Recherche Scientifique, 45071 Orléans Cedex 2, France

E-mail: gerard.le-caer@univ-rennes1.fr, bruno.bureau@univ-rennes1.fr and dominique.massiot@cnrs-orleans.fr

Received 8 October 2009, in final form 5 January 2010
Published 22 January 2010
Online at stacks.iop.org/JPhysCM/22/065402

Abstract

First, the basis and the characteristics of the Czjzek model for the distribution of electric field gradient (EFG) tensor in disordered solids, some of which are still unnoticed, are depicted. That model results from the statistical invariance by rotation of the structure of the considered disordered solid and from the applicability of a central limit theorem to the EFG tensor. These two conditions, which are physically realistic for a wealth of disordered solids, simplify tremendously the derivation of the EFG distribution but at the cost of a complete loss of structural information about the investigated solid. Next, we describe a simple extension of it which is intended to mimic a well-defined local environment, with given values of the asymmetry parameter and of the principal component V_{zz} of the EFG tensor, perturbed by the disorder of more remote atoms. The effect of disorder is rendered by a Gaussian (Czjzek) noise with an adjustable weight relative to V_{zz}. The number of free parameters is limited to three, as compared to a sole scale factor for the Czjzek model. Its characteristics are described as a function of the given asymmetry parameter and of the strength of the noise. The aim is to lead to a practical tool which may help to retrieve, as far as possible, the information about the local environment perturbed by disorder from hyperfine measurements and notably from NMR spectra of quadrupolar nuclei. As an example, that extension is applied to some static NMR spectra of ^{71}Ga in covalent glasses. Calculated static ^{71}Ga NMR lineshapes are shown as a function of the parameters of the extended model.

(Some figures in this article are in colour only in the electronic version)

1. Introduction

The distributions of electric field gradients at the nuclei of a variety of isotopes are very often studied by hyperfine techniques, such as nuclear solid state nuclear magnetic resonance (NMR), nuclear quadrupole resonance (NQR), perturbed angular correlations (PAC), and Mössbauer spectroscopy, to gain information on disordered materials, both crystalline and non-crystalline. Electron paramagnetic

[4] Author to whom any correspondence should be addressed.

resonance (EPR), the concepts of which are similar to those of NMR, is quite naturally added to the previous non-exhaustive list.

Czjzek *et al* [1] proposed a model which has played a seminal role in the analysis of the EFG distribution of random atomic arrangements. The Czjzek model provides a joint probability distribution $f_{\mathrm{C}}(V_{zz}, \eta)$ of the principal value V_{zz} of the EFG tensor and of the classical asymmetry parameter η. The latter is redefined in section 2.1 and is equally denoted by η_Q in the NMR literature, as done hereafter when relevant. The density probability $f_{\mathrm{C}}(V_{zz}, \eta)$ yields the probability $f_{\mathrm{C}}(V_{zz}, \eta)\,\mathrm{d}V_{zz}\,\mathrm{d}\eta$ that V_{zz} and η range simultaneously between V_{zz} and $V_{zz} + \mathrm{d}V_{zz}$ and between η and $\eta + \mathrm{d}\eta$, respectively. The very same EFG distribution was independently derived by Stöckmann [2] for a cubic system with a large concentration of vacancies randomly distributed.

As emphasized recently by d'Espinose de Lacaillerie *et al* [3], the relation between structural data and the quadrupolar interaction is obtained in the best situation by *ab initio* calculations of the EFG. The situation is however much more complex when dealing with materials which are neither perfectly nor almost perfectly ordered. In the presence of a significant disorder, the quadrupolar interactions reflect the statistical distribution of the EFG, which require modelling from the structural disorder at the relevant scale. The latter task is complex, as it is for modelling almost all physical properties of such materials, but disorder is fortunately a source of simplification when the physics which determines the considered property makes possible the application of a central limit theorem (CLT). The importance of the Czjzek model, whose general conditions of validity were discussed by Le Caër *et al* [4–7], stems indeed from the fact that it is an attraction basin of many EFG tensor distributions in disordered solids. This results from the application of a CLT [8] to the five-dimensional vector (section 2.1) which is necessary to define completely a symmetric, zero-trace EFG tensor whose distinct elements are sums over a large number of random terms with various physical origins. The central limit theorem applies when every term of a given sum of random variables has a reduced importance if considered individually (see among others [8] for precise and rigorous formulations). The fact that the Czjzek model results just from the two very general assumptions discussed below, statistical isotropy [1] and validity of the conditions of application of the CLT [4, 5], was not immediately recognized and, for some time, that model was considered as being a way to test the adequacy of dense random packing models [9]. By that was more precisely meant a dense random packing of hard spheres (RDPHS, Bernal model). The validity of the Czjzek model for a non-relaxed cubic solid with a high density of vacancies [2], which is a clear counter-example of the latter conclusion, was ignored for some years. It is therefore not surprising that the measured quadrupolar interactions lose all specific information about the disordered structure from which they originate and provide a single scale parameter when the Czjzek model holds. The latter parameter may however be of physical interest for the characterization of various solids. Although physics seems to be absent from the Czjzek model, it is worth emphasizing that theoretical calculations of the EFG are needed to establish which general conditions on structures and chemical bonding favour that model.

The Czjzek model is supported by two pillars, as discussed in detail in [7] (see further section 2.1).

(1) The first is the statistical invariance by rotation of the structure of the considered disordered solid [1]. That condition must not be misconceived as the statistical isotropy of the EFG tensor does not imply any local structural isotropy of the latter solid.
(2) The second is the aforementioned applicability of the central limit theorem to the EFG tensor elements [4]. A random EFG tensor whose elements fulfil the two conditions of validity of the Czjzek model will be named hereafter a Czjzek tensor.

The most general idea on the structure of amorphous solids is that they are isotropic on average. The first condition thus appears rather straightforward. It may however be noticed that deviations from an overall isotropy were reported to occur in deformed glasses ([10–12] and references therein). They were either studied by x-ray diffraction experiments in metallic glasses [10] or by molecular dynamics simulations in metallic glasses [11] and in silica glass [12]. The second condition is more dependent on the nature of the investigated materials than is the first one. If the Czjzek model does not hold, more must be known about the considered materials, their atomic structure and their electronic structure to obtain a trustworthy EFG model. Obtaining a general model which differs from the Czjzek model thus seems hopeless.

A simple extension of the Czjzek model was nevertheless introduced first in [5] in relation to ^{57}Fe quadrupole splitting distributions, and then investigated partly in [7]. That model was intended to mimic the EFG tensor of a well-defined neighbourhood of a given atomic species perturbed by a 'random noise' tensor which reflects the effect of disorder in more remote atomic shells. The total EFG tensor is then the sum of a fixed EFG tensor, with a given principal value $V_{zz}(0)$ and a given asymmetry parameter η_0, and of a Czjzek tensor whose weight is proportional to a tunable parameter ε. The evolution of the characteristics of the total tensor was investigated in [7], more particularly for $\eta_0 = 0$, as a function of ε to determine the minimum value of it for which the Czjzek noise outweighs the constant EFG to a point where the effect of the latter is essentially hidden. The emphasis in [7] was then put on large values of the parameter ε. This model is worth reinvestigating for all values of η_0 and, more particularly, for small to moderate values of ε. It may indeed be of some interest in NMR, which is a widely used structural tool in solid state sciences, especially for characterizing disordered or complex materials. The lineshape of the many nuclei whose spin is $I > 1/2$, ^{7}Li, ^{11}B, ^{23}Na, ^{27}Al, ^{69,71}Ga, ^{133}Cs to name just a few, is dominated by the quadrupolar interaction. The latter interaction results from the coupling between the nuclear quadrupole moment Q with the EFG created by the surrounding electric charges. The NMR lineshapes then depend on the asymmetry parameter η_Q and on the quadrupolar frequency, $\nu_Q = \frac{3|eQV_{zz}|}{2I(2I-1)}$ where I and Q are respectively the

nuclear spin and the nuclear quadrupole moment of the ground state. To account for any NMR spectrum of a quadrupolar nucleus in a disordered solid thus requires one to rely on some distribution $f(\nu_Q, \eta_Q)$, or equivalently on $f(V_{zz}, \eta)$. One of the aims of the present extension of the Czjzek model is thus to investigate a distribution which might be of some use in accounting for the actual NMR spectra of disordered solids.

In the following, we shall first recall the characteristics of the Czjzek model which are needed for a self-contained description of the extended model and to pose the questions which are addressed in the present work. Some unpublished characteristics of the Czjzek distribution of V_{zz} and η, which are useful in the present context, shall be given. Then, we shall characterize the extended Czjzek model as a function of its parameters with the aim of obtaining results in a convenient form and of defining a practical method of application of the model. Finally, we shall exhibit NMR lineshapes to evidence the influence of ε in the whole range and we shall show how such a model applies to the ^{71}Ga NMR spectrum of a glass of the binary system GeS_2–Ga_2S_3.

2. The Czjzek model

For simplicity, almost all probability distributions used in the present work will be denoted as $p_C(x)$, $p_E(x)$ for the univariate distribution of a physical observable x which may be V_{zz}, η or $\Delta = |V_{zz}|\sqrt{1+\eta^2/3}$ and $p_C(x, y)$, $p_E(x, y)$ for the distribution of couples (x, y) of physical quantities, for instance (V_{zz}, η) or (Δ, η). The lower indices C and E refer respectively to the Czjzek model and to its extension. The use of a single notation $p_A(\ )$ for distributions whose functional forms differ, $p_A(x) \neq p_A(y)$ if $x \neq y$ is not really confusing, as it is the nature of the variable x itself which makes it clear which distribution $p_A(x)$ is being dealt with.

2.1. The basic ingredients

The elements of the EFG tensor $\bar{\boldsymbol{V}}$ in its general non-diagonal form are written in lower case $(v_{ij}, i, j = x, y, z)$. If the principal values of the EFG tensor, denoted in upper case as $V_{xx}, V_{yy}, V_{zz} (V_{xx} + V_{yy} + V_{zz} = 0)$, are sorted such that $|V_{xx}| \leqslant |V_{yy}| \leqslant |V_{zz}|$, the asymmetry parameter is recalled to be defined as: $0 \leqslant \eta = \frac{V_{xx}-V_{yy}}{V_{zz}} \leqslant 1$.

Considerations about the distribution of the EFG tensor itself and not only about the distribution of its eigenvalues (through the bivariate distribution of V_{zz} and η) are of interest in disordered solids because additivity of the various physical contributions holds for the elements of the EFG tensor, but not for its eigenvalues. The distribution of the EFG tensor cannot be directly accessed by experiments, but the consequences of assumptions about it can be. Following Czjzek *et al* [1], we define a five-dimensional real vector, $\boldsymbol{U} = (U_1, U_2, \ldots, U_5)$, deduced from the irreducible spherical tensor associated with any zero-trace symmetric second-rank tensor, as is the EFG tensor $\bar{\boldsymbol{V}}$. Its irreducible components, which transform as linear combinations of spherical harmonics of degree 2, are given by: $U_1 = v_{zz}/2, U_2 = v_{xz}/\sqrt{3}, U_3 = v_{yz}/\sqrt{3}, U_4 = v_{xy}/\sqrt{3}, U_5 = (v_{xx} - v_{yy})/(2\sqrt{3})$. The latter tensor can then be written as

$$\bar{\boldsymbol{V}} = \begin{bmatrix} -U_1 + U_5\sqrt{3} & U_4\sqrt{3} & U_2\sqrt{3} \\ U_4\sqrt{3} & -U_1 - U_5\sqrt{3} & U_3\sqrt{3} \\ U_2\sqrt{3} & U_3\sqrt{3} & 2U_1 \end{bmatrix}. \quad (1)$$

The second invariant of the EFG tensor is thus proportional to the square of the norm, of the vector $\boldsymbol{U}(\mathrm{tr}(\bar{\boldsymbol{V}}^2) = 6\|\boldsymbol{U}\|^2 = \frac{3}{2}V_{zz}^2(1 + \frac{\eta^2}{3}) = \frac{3}{2}\Delta^2)$, where tr means 'trace'. The latter vector is also the addition of physical contributions of various origins and is thus a random vector in a disordered solid. It is thus equivalent to consider the distribution of the EFG tensor or the distribution of the vector $\boldsymbol{U}$, which will be named the EFG vector. Both will equally be dealt with in the following. If the considered disordered solid is statistically invariant by any rotation, then the five components of $\boldsymbol{U}$ fulfil a number of conditions, the relevant and essential ones being [7]

$$\begin{cases} \langle U_k \rangle = 0 \\ \langle U_j U_k \rangle = \sigma^2 \delta_{jk} \end{cases} \qquad (k = 1, \ldots, 5), \quad (2)$$

where $\langle X \rangle$ denotes the average of the random variable X. The covariance matrix $\boldsymbol{\Lambda}$, whose elements $\Lambda_{ij} (i, j = 1, \ldots, 5)$ are $\langle U_i U_j \rangle$ because the means are zero, is proportional to a unit 5×5 matrix, $\boldsymbol{\Lambda} = \sigma^2 \boldsymbol{I}_5$. The U_ks are therefore uncorrelated random components, but in general this does not mean that they are independent. For a statistically isotropic solid, the marginal distributions $p(U_k)$, $k = 2, \ldots, 5$ were further shown to be identical and symmetric [7]. By contrast, the distribution of $p(U_1)$ is in general different from the latter, being *a priori* asymmetric with a zero mean (equation (2)) [7]. The most general form of the distribution of $\boldsymbol{U}$, associated with a statistically invariant EFG tensor, was shown to be given by $p_{SI}(\boldsymbol{U}) = p_{SI}(\|\boldsymbol{U}\|, \det(\bar{\boldsymbol{V}}))$ where det means determinant [1]. When $p_{SI}(\boldsymbol{U})$ is a sole function of $\|\boldsymbol{U}\|$, then the distribution of $\boldsymbol{U}$ is spherical in 5D, that is invariant by any five-dimensional rotation. We notice that a 5D invariance of the EFG vector distribution implies its invariance in 3D but the converse is generally untrue.

The distribution of $\boldsymbol{U}$ is multivariate Gaussian in all cases where the physics that determines the EFG distribution meets the requirements of the multidimensional central limit theorem [8]. In that case, none of the random contributions to the components of the total EFG dominates the others. They fulfil the so-called uniform smallness condition, which is a consequence of the general conditions of validity of the CLT. The two conditions, statistical isotropy and applicability of the central limit theorem, imply in addition that the U_ks are now independent and identically distributed Gaussian random variables with a mean zero and a variance σ_C^2 [7], because $\boldsymbol{\Lambda} \propto \boldsymbol{I}_5$. In the latter case, the Gaussian tensor $\bar{\boldsymbol{V}}$ will be denoted by $\bar{\boldsymbol{V}}_C$ (the evocative name Gaussian isotropic (GI) will be used too). The two previous GI conditions then determine a unique reference random tensor $\bar{\boldsymbol{V}}_C$, but for a scaling factor σ_C which is characteristic of the investigated solid. The distribution of

$\boldsymbol{U}_C$:

$$p_C(\boldsymbol{U}_C) = p_C(U_{C1}, U_{C2}, \ldots, U_{C5}) = \frac{1}{(2\pi\sigma_C)^5}\exp\left(-\frac{\sum_{k=1}^{5} U_{Ck}^2}{2\sigma_C^2}\right) = \frac{1}{(2\pi\sigma_C)^5}\exp\left(-\frac{\|U_C\|^2}{2\sigma_C^2}\right) \quad (3)$$

is thus seen to be invariant not only by any rotation in 3D but more generally by any orthogonal transformation in 5D.

The Czjzek model is a well-defined universal reference state for both the EFG tensor and the EFG vector distributions. It holds more generally for any symmetric, zero-trace second-rank tensor, whose elements are also sums of random physical contributions, which fulfils the two conditions discussed above. This is, for instance, the case of the deviatoric atomic level stress (ALS) tensor. The ALS tensor was defined by Egami *et al* ([13, 14] and references therein) for every atom of a solid. It can be calculated from the knowledge of interatomic potentials. The elements of the ALS tensor at any atomic position in a disordered structure are then sums of contributions from the surroundings of the considered site. An analysis which parallels that done for the Czjzek model can then be directly applied to the ALS tensor in a disordered solid, as shown in [4]. It is worth noticing that the von Mises shear stress [13, 14] and the quadrupole splitting, measured for instance in ^{57}Fe and ^{119}Sn Mössbauer spectroscopy, which are proportional to the norm of the ALS tensor and of the EFG tensor respectively, then both have the same distribution ($p(x) \propto x^4\exp(-a^2x^2)$, section 2.2). The irreducible elements of the EFG tensor are equivalent to the second-order crystal field terms in the Hamiltonian which describes the interaction between local electronic states and the potential of surrounding charges [9, 15]. Properties which are sensitive to crystal fields were thus calculated using the functional form of the Czjzek model [15]. Significant deviations from the Czjzek model were reported for rare-earth amorphous alloys, from which it was concluded that the distribution of local symmetries is not consistent with RDPHS's [15].

Finally, it is worth mentioning that the random EFG vector, $\boldsymbol{U}_C$, is the vector that has the largest Shannon entropy (named differential entropy for continuous random variables), $S[p] = \int_{\mathbb{R}^5} p(\boldsymbol{U})\ln(p(\boldsymbol{U}))\,\mathrm{d}\boldsymbol{U}$, over all random vectors with the sole constraints of a zero mean vector $\langle\boldsymbol{U}\rangle = 0$ and of a given covariance matrix, $\boldsymbol{\Lambda} = \sigma^2\boldsymbol{I}_5$, which hold here as a consequence of statistical isotropy (equation (2)). Further, using spherical coordinates, the Czjzek distribution is easily shown to be the maximum entropy distribution among all spherical distributions which have a density $p_S(\|\boldsymbol{U}\|)$ with the constraint that $\langle\|\boldsymbol{U}\|^2\rangle = 5\sigma^2$. The most general isotropic distribution, with a density given by $p_{SI}(\|\boldsymbol{U}\|, \det(\bar{\boldsymbol{V}}))$, however, not only obeys the two constraints given by equation (2) but supplementary constraints [1, 7]. These additional constraints are evidently satisfied by the spherical distributions considered above. Following Jaynes [16], a maximum entropy distribution is 'maximally noncommittal', meaning as uniform as it can be without violating the given constraints. The previous discussion then suggests that the additional constraints, if they are nonredundant with those given by equation (2), decrease the entropy of an isotropic distribution with respect to that of the Czjzek distribution. Consistently, the CLT can be viewed as a 'maximum entropy' result [17].

2.2. Some characteristics of the distribution $f_C(V_{zz}, \eta)$

When an EFG tensor reduces to a Czjzek tensor, the observed distributions have universal functional forms and detailed structural information cannot be gained from them as discussed in section 1. To establish a direct link between the multivariate Gaussian distribution $p_C(\boldsymbol{U}_C)$ (equation (3)) and the distributions of the eigenvalues of $\bar{\boldsymbol{V}}_C$, we have chosen σ_C as the scaling factor and not $\sigma(=2\sigma_C)$ as done in [7]. The bivariate distribution $f_C(V_{zz}, \eta)$ is then [1, 7]

$$f_C(V_{zz}, \eta) = \eta\left(1 - \frac{\eta^2}{9}\right)\frac{V_{zz}^4}{32\sigma_C^5\sqrt{2\pi}} \times \exp\left(-\frac{V_{zz}^2}{8\sigma_C^2}\left(1 + \frac{\eta^2}{3}\right)\right) \quad (4)$$

which yields the distribution of η [1]:

$$p_C(\eta) = \frac{3\eta\left(1 - \frac{\eta^2}{9}\right)}{\left(1 + \frac{\eta^2}{3}\right)^{5/2}} \quad (5)$$

whose average value and standard-deviation are respectively, $\langle\eta\rangle_C = 2\sqrt{3} - (3\sqrt{3}/2)\ln 3 = 0.609\,823\ldots$ and $\sigma_{\eta,C} = 0.242\,685\ldots$. As the frequency ν_Q is proportional to $|V_{zz}|$, the sign of V_{zz} is irrelevant to the present work. We restrict then the domain of integration of $f_C(V_{zz}, \eta)$ and therefore below we use $p_C(V_{zz}, \eta) = 2f_C(V_{zz}, \eta)(V_{zz} \geqslant 0, 0 \leqslant \eta \leqslant 1)$.

Equation (4) shows that V_{zz} and η are not independent but that they are weakly correlated. The only term which is responsible for a correlation between them is indeed the $(1 + \eta^2/3)$ factor in the exponential, which ranges between 1 and $\approx$1.1547. This is better seen by calculating the conditional distributions $p_C(v|\eta_1 \leqslant \eta \leqslant \eta_2)$ and $p_C(\eta|v_1 \leqslant v \leqslant v_2)$, where $p_C(x|y_1 \leqslant y \leqslant y_2)$ is the density probability of x knowing that $y_1 \leqslant y \leqslant y_2$ ($y_2 - y_1 \geqslant \mathrm{d}y$). The conditional distribution $p_C(v|\eta_1 \leqslant \eta \leqslant \eta_2)$ varies as $\propto v^4$ when $v \to 0$ for any pair such that $0 \leqslant \eta_1 < \eta_2 \leqslant 1$ (unpublished results). The correlation coefficient between η and $|V_{zz}|$ is calculated to be ≈ -0.1241. By contrast, η and $\Delta = |V_{zz}|\sqrt{1 + \eta^2/3}$, which is proportional to the norm of the EFG tensor ($\|\boldsymbol{V}_C\| = \sqrt{\mathrm{tr}\,\boldsymbol{V}_C^2} = (\sum_{i,j=x,y,z} v_{Cij}^2)^{1/2} = \Delta\sqrt{3/2}$), are independent random variables. The latter quantity is proportional to the quadrupole splitting that is measured for instance by ^{57}Fe and ^{119}Sn Mössbauer spectroscopy in the non-magnetic state of solids. We obtain from $p_C(V_{zz}, \eta)$ that

$$p_C(\Delta, \eta) = \frac{3\eta(1 - \eta^2/9)}{(1 + \eta^2/3)^{5/2}}\frac{\Delta^4}{48\sigma_C^5\sqrt{2\pi}}\exp\left(-\frac{\Delta^2}{8\sigma_C^2}\right) = p_C(\eta)p_C(\Delta). \quad (6)$$

Equation (6) justifies the use of polar coordinates to plot the contour maps of the Czjzek distribution (see [1] and

figures 2 and 9 of [7]). The functional form of the quadrupole splitting distribution often used in Mössbauer spectroscopy is consistently taken to be $p_C(\Delta)$. The distribution $p_C(\Delta)$ is obtained in a different way just by noticing that $\frac{\Delta}{2\sigma_C} = \sqrt{\sum_{k=1}^{5} \frac{U_{Ck}^2}{\sigma_C^2}}$ has, by definition, a chi distribution with five degrees of freedom [8, 18].

To describe simply how η can be independent of Δ, we express $\boldsymbol{U}_C$ as $\boldsymbol{U}_C = \|\boldsymbol{U}_C\|\boldsymbol{u}_C = (\Delta/2)\boldsymbol{u}_C$, where $\boldsymbol{u}_C$ is a 5D unit vector. Equation (3) shows that the distribution of the Gaussian vector $\boldsymbol{U}_C$ is spherical, as it depends only on its norm. Then, the distribution of the unit vector $\boldsymbol{u}_C = \boldsymbol{U}_C/\|\boldsymbol{U}_C\|$ is isotropic, that is, its tip spans uniformly the surface of the 5D unit sphere (see for instance section V.4 of [18]). We then consider an arbitrary unit vector that we fix, $\boldsymbol{u}_C(f)$, and the tensor $\bar{\boldsymbol{V}}(f) = \bar{\boldsymbol{V}}(\boldsymbol{u}_C(f))$ obtained from it by applying equation (1) as well as its principal values. The elements of the EFG tensor calculated from $\boldsymbol{U}_C(f) = (\Delta/2)\boldsymbol{u}_C(f)$, where Δ has now an arbitrary value, and its principal values are then those of $\bar{\boldsymbol{V}}(f)$ multiplied by $\Delta/2$. This leaves $\eta_f = \eta(\boldsymbol{u}_C(f))$ unchanged, as it is a ratio of principal values. Selecting a vector whose orientation is kept constant for any radius thus yields a single value of η_f for any Δ. The distribution of η of the Czjzek model is thus fully determined by the uniform distribution on the surface of a 5D sphere independently of its radius $\propto\Delta$. Actually, the latter distribution is still obtained if the unit vector is uniformly distributed only on one eighth of the surface. More generally, an EFG vector distribution, associated with an EFG tensor statistically isotropic in 3D, for which $\boldsymbol{U} = \|\boldsymbol{U}\|\boldsymbol{u} = (\Delta/2)\boldsymbol{u}$, may give rise to a distribution $p(\Delta, \eta)$ with independent η and Δ as soon as the distribution of $\boldsymbol{u}$ is independent of Δ. However, the resulting distribution of η has no reason to coincide with $p_C(\eta)$ (equation (5)) for any anisotropic distribution of the 5D unit vector $\boldsymbol{u}$.

Another way of expressing the independence of η and Δ is through a so-called stochastic representation of $\boldsymbol{U}$, $\boldsymbol{U} \stackrel{d}{=} R\boldsymbol{u}$, where $A \stackrel{d}{=} B$ means that A and B are identically distributed and where the random variable R and the 5D random vector $\boldsymbol{u}$ are independent. Generating a uniformly distributed 5D unit vector $\boldsymbol{u}_C$ by Monte Carlo simulation, and using its components to construct a tensor, yields $p_C(\eta)$ (equation (5)) as expected. The distribution $p_C(\eta)$ is then obtained for all distributions of the form $p(\Delta, \eta) \propto p_C(\eta)G(\Delta^2)$ [7]. As observed experimentally, the distribution $p_C(\eta)$ is robust and holds in a variety of conditions which deviate from those of the Czjzek model (also see section 4). The appendix describes a different approach to the EFG tensor and to $p_C(\eta)$ based on a Maxwell multipole [19, 20].

Further characteristics of the Czjzek model which are relevant to the present work are given below. The distribution of $v = |V_{zz}|$ is [4]

$$p_C(v) = \frac{1}{\sigma_C}\sqrt{\frac{2}{\pi}}\left[\left(\frac{3v^2}{8\sigma_C^2} - 1\right)\exp\left(-\frac{v^2}{8\sigma_C^2}\right) + \left(1 - \frac{v^2}{3\sigma_C^2}\right)\exp\left(-\frac{v^2}{6\sigma_C^2}\right)\right] \qquad v > 0 \tag{7}$$

with a maximum at $3.734\,206\,82\ldots\sigma_C$, an unpublished value of the ratio of the full width at half maximum to the position of the maximum of $0.831\,254\,2367\ldots$ and a variation $\propto v^4$ when $v \to 0$. The first two moments of v are $\langle|V_{zz}|\rangle = 5\sigma_C\sqrt{2/\pi}$ and $\langle|V_{zz}|^2\rangle = \sigma_C^2(28 - 6\sqrt{3})$, from which the ratio $\sigma_{|V_{zz}|}/\langle|V_{zz}|\rangle$ is deduced to be $\sqrt{14\pi - 3\pi\sqrt{3} - 25}/5 = 0.326\,07\ldots$ [4], where $\sigma_{|V_{zz}|} = \sqrt{\langle|V_{zz}|^2\rangle - \langle|V_{zz}|\rangle^2}$.

2.3. The Czjzek model $C(n)$

A model, named here $C(n)$, was proposed by Czjzek [21] to generalize the distribution of Δ found for the previous Czjzek model ($n = 5$) to distributions of the form $p_{C(n)}(\Delta) = \frac{\Delta^{n-1}}{2^{(n-2)/2}\sigma^n\Gamma(n/2)}\exp(-\frac{\Delta^2}{2\sigma^2})$, $(n = 1, \ldots, 4)$. That extension was intended to account for distributions of ^{57}Fe quadrupole splitting of the type were reported to occur in ionic glasses and in metallic glasses. For that purpose, Czjzek made another assumption on the distribution of the EFG tensor. He assumed that the five components of the vector $\boldsymbol{U}$ (section 2.1) are not independent and that they are linear functions of $n(<5)$ Gaussian random variables with a zero mean [21]. The main consequence of that (ad hoc) assumption is that the distribution of the EFG tensor is no longer invariant by rotation, a fact which went largely unnoticed [7]. Indeed, the covariance matrix $\boldsymbol{\Lambda}$ is now singular by construction while it must be proportional to a unit 5×5 matrix in the case of statistical isotropy (equation (2)). It is easy to exhibit a statistically isotropic distribution of the EFG vector which yields $p_{C(n)}(\Delta)$. By the results of section 2.1, the distribution of $\boldsymbol{U}$ cannot be multivariate Gaussian ($n < 5$) because the unique multivariate Gaussian distribution consistent with isotropy is that of Czjzek's model with $n = 5$. The proposed EFG vector distribution is simply given by $p_{C(n)}(\boldsymbol{U}) \propto (\sum_{k=1}^{5} U_k^2)^{(n-5)/2}\exp(-\sum_{k=1}^{5} U_k^2/2\sigma^2)$. The common distribution of the U_ks is given by $p_n(U_k) \propto \exp(-U_k^2/2\sigma^2) \times \int_0^\infty x\exp(-x/(2\sigma^2))\,\mathrm{d}x/(x + U_k^2)^{(5-n)/2}$. The associated distribution $p_{C(n)}(|V_{zz}|, \eta)$ is $\propto\eta(1 - \eta^2/9)(1 + \eta^2/3)^{(n-5)/2} \times |V_{zz}|^{n-1}\exp(-V_{zz}^2(1 + \eta^2/3)/8\sigma^2)$ and the distribution of the asymmetry parameter is still $p_C(\eta)$ (equation (5)) because the distribution $p_{C(n)}(\boldsymbol{U})$ is spherical in 5D (section 2.2).

An empirical bivariate distribution, inspired both by $p_C(|V_{zz}|, \eta)$ and by $p_{C(n)}(\Delta)$ and for that reason still named Czjzek's model, $p_n(|V_{zz}|, \eta) \propto \eta(1 - \frac{\eta^2}{9}) \times |V_{zz}|^{n-1}\exp(-\frac{V_{zz}^2}{2\sigma^2}(1 + \frac{\eta^2}{3}))$, was used to interpret EPR or NMR spectra (see for instance [22–25]). If the latter model is intended to be associated with a statistically isotropic disordered solid then, as discussed above, the distribution of $\boldsymbol{U}$ cannot be multivariate Gaussian and the distribution of the associated EFG vector cannot fulfil the basic assumption of the Czjzek's extension with $n < 5$. The name that model bears then all the more confuses that the $p_n(|V_{zz}|, \eta)$ distribution may have practical interest [22–25]. The distribution of η which is associated to $p_n(|V_{zz}|, \eta)$ is easily found to be $p_n(\eta) \propto \eta(1 - \eta^2/9)/(1 + \eta^2/3)^{n/2}$. A model, which gives rise to $p_n(|V_{zz}|, \eta)$, still remains to be displayed and constructed on a reasoned basis.

3. A simple extension of the Czjzek model

The Czjzek model is, so to speak, a kind of 'black hole' out of which no information about the specific structural features

of the investigated solid and about the physical origins of the EFG can come. The extended model discussed here is then motivated by the recovery of the structural information, contained in the EFG about short-range order in a disordered solid, eclipsed partly by a Gaussian noise which tends to absorb that information. The model is intended to mimic the EFG contribution of a well-defined neighbourhood of a given atomic species modified by the effect of more remote atomic shells. Actually, it would suffice that some close neighbourhood gives rise to an EFG tensor with fixed values of $\eta = \eta_0$ and of $V_{zz} = V_{zz}(0)$. The proposed extension of the Czjzek model then reads

$$\bar{\boldsymbol{V}}_{\mathrm{E}}(\varepsilon) = \bar{\boldsymbol{V}}(0) + \rho(\varepsilon)\bar{\boldsymbol{V}}_{\mathrm{C}} \qquad (\varepsilon, \rho(\varepsilon) > 0). \tag{8}$$

For the sake of simplicity, the explicit dependence of ρ on ε will be dropped hereafter. One aim is to provide a sufficiently realistic and possibly practical model while keeping the number of free parameters as small as possible. In equation (8), the EFG tensor $\bar{\boldsymbol{V}}_{\mathrm{E}}(\varepsilon)$ is the sum of two parts, the first one being a fixed diagonal tensor $\bar{\boldsymbol{V}}(0)$:

$$\bar{\boldsymbol{V}}(0) = \begin{bmatrix} V_{zz}(0)(\eta_0 - 1)/2 & 0 & 0 \\ 0 & -V_{zz}(0)(\eta_0 + 1)/2 & 0 \\ 0 & 0 & V_{zz}(0) \end{bmatrix} \tag{9}$$

which is associated with a vector $\boldsymbol{U}(0) = (V_{zz}(0)/2, 0, 0, 0, \eta_0 V_{zz}(0)/2\sqrt{3})$ and characterized by an asymmetry parameter η_0 and a principal value $V_{zz}(0)$. The second part is a random 'noise 'tensor $\bar{\boldsymbol{V}}_{\mathrm{RN}}$, taken to be a Czjzek tensor, namely $\bar{\boldsymbol{V}}_{\mathrm{RN}} = \rho\bar{\boldsymbol{V}}_{\mathrm{C}}$, with a 'weight' ρ proportional to ε defined below by equation (10). The tensor $\bar{\boldsymbol{V}}_{\mathrm{C}}$ is obtained from equation (1), from a vector $\boldsymbol{U}_{\mathrm{C}} = (U_{\mathrm{C}1}, U_{\mathrm{C}2}, \ldots, U_{\mathrm{C}5})$, whose five components are identically and independently distributed Gaussian variables with $\langle U_{\mathrm{C}k}\rangle = 0$ and a variance chosen here to be $\sigma_{\mathrm{C}}^2 = \langle U_{\mathrm{C}k}^2\rangle = 1$ $(k = 1, \ldots, 5)$ (equation (3)). That simple choice reduces the number of adjustable parameters to three, $V_{zz}(0)$, ε and η_0.

3.1. Statistical isotropy

As $\bar{\boldsymbol{V}}_{\mathrm{RN}}$ is statistically invariant by any rotation, it is possible to chose the frame of reference in which $\bar{\boldsymbol{V}}(0)$ is set to be diagonal without loss of generality. The latter choice is indeed not inconsistent with the possible existence of an amorphous solid, statistically invariant by rotation, whose local EFG distribution would be given by equation (8). Let us consider the example of an amorphous solid in which a given atomic species has a well-defined first coordination shell (to within small deformations) while atomic positions of more remote atoms fluctuate. An example of an amorphous structure, which might be described in that way, is that of $GeSe_4$, obtained by molecular dynamics, which is shown in figure 1 of [26] although its EFG distribution is not claimed to agree with equation (8) (see further section 5). This amorphous solid is isotropic on average, from the point of view of the selected atomic species probed by hyperfine techniques, if the tips of unit vectors of a local frame of reference of the 'cluster' formed by the central atom and its neighbours span uniformly a unit sphere. In other words, it would suffice to rotate uniformly the frame of reference of the local EFG tensor to obtain the actual EFG tensor distribution of the whole amorphous solid in a laboratory reference frame, fixed for all atoms whose EFG is studied. The latter EFG distribution is not explicitly given here, but it cannot be accessed experimentally. In any case, the distribution of that tensor cannot be multivariate Gaussian because, in that case, statistical isotropy would lead unavoidably to Czjek's model (sections 2.1 and 2.3). Only quantities related to the distribution of the principal values can be measured and are considered here. The relevant physics is contained in the ensemble of configurations described by $\bar{\boldsymbol{V}}_{\mathrm{RN}}$ in the frame of reference of the fixed part $\bar{\boldsymbol{V}}(0)$, that is in the frame of reference of a local 'cluster'. Rotating the latter frame uniformly in all directions would be useless, as it would not change the distribution $p_{\mathrm{E}}(V_{zz}, \eta)$ derived directly from equation (8). That operation would be of interest only in the case where a structural model provides the EFG tensor distribution, which might then be compared to that of the extended model. The appendix provides a way to obtain the EFG tensor distribution from Monte Carlo simulations.

The previous arguments on statistical isotropy might apply to the extension of Czjzek's model, $C(n)$ [21], discussed in section 2.3 with the restricting condition that the correlated Gaussian components of $\boldsymbol{U}$ are now local ones and not global ones. The distribution $p_{\mathrm{C}(n)}(\Delta)$ would be recovered by hypothesis but the associated distribution of η has no reason to conform with the unique distribution $p_n(\eta)$ associated to a given n (section 2.3). The distribution of η would depend instead on the covariance structure chosen for the U_ks $(k = 1, \ldots, 5)$, which is a key ingredient of such a model (see p 10734 of [7]).

3.2. The explicit total EFG tensor

The proposed extension might have been simply phrased as 'two components of the EFG vector, U_1 and U_5, of the Czjzek model are given non-zero means'. The formulation given by equation (8) was chosen here to make more clear physical and structural interpretations of it. If, for a given value of η_0, $V_{zz}(0)$ is multiplied by α, then all elements of $\bar{\boldsymbol{V}}(0)$ are multiplied by α. The norm $M_0 = \sqrt{\mathrm{tr}\,\bar{\boldsymbol{V}}^2(0)} = \sqrt{\frac{3}{2}}|V_{zz}(0)|\sqrt{1 + \eta_0^2/3}$ and thus ρ (equation (10)) are then both multiplied by α. The tensor $\bar{\boldsymbol{V}}_{\mathrm{E}}(\varepsilon)$ becomes then $\alpha\bar{\boldsymbol{V}}_{\mathrm{E}}(\varepsilon)$ while the associated asymmetry parameter remains the same: $V_{zz}(0)$ is just a scaling factor which is taken as equal to 1 in the Monte Carlo simulations of section 4. The mean second invariant of $\bar{\boldsymbol{V}}_{\mathrm{C}}$, $M_{\mathrm{C}}^2 = \langle \mathrm{tr}\,\bar{\boldsymbol{V}}_{\mathrm{C}}^2\rangle$, is then easily found from equation (2) to be $M_{\mathrm{C}}^2 = \langle 6\sum_{k=1}^{5} U_{\mathrm{C}k}^2\rangle = 30$. The perturbation ε is defined to be the ratio of M_{RN}, defined by $M_{\mathrm{RN}}^2 = \langle \mathrm{tr}\,\bar{\boldsymbol{V}}_{\mathrm{RN}}^2\rangle = \rho^2 M_{\mathrm{C}}^2$, to the norm of $\bar{\boldsymbol{V}}(0)$, $M_0 = \sqrt{\mathrm{tr}\,\bar{\boldsymbol{V}}^2(0)} = \sqrt{\frac{3}{2}}|V_{zz}(0)|\sqrt{1 + \eta_0^2/3}$. The weight ρ is then

$$\varepsilon = \frac{M_{\mathrm{RN}}}{M_0} = \frac{\rho\sqrt{30}}{M_0} \Rightarrow \rho = \frac{M_0\varepsilon}{\sqrt{30}}. \tag{10}$$

The total tensor can then be written as

$$\bar{\boldsymbol{V}}_{\mathrm{E}}(\varepsilon) = \begin{bmatrix} V_{\mathrm{E}11} & \rho U_{\mathrm{C}4}\sqrt{3} & \rho U_{\mathrm{C}2}\sqrt{3} \\ \rho U_{\mathrm{C}4}\sqrt{3} & V_{\mathrm{E}22} & \rho U_{\mathrm{C}3}\sqrt{3} \\ \rho U_{\mathrm{C}2}\sqrt{3} & \rho U_{\mathrm{C}3}\sqrt{3} & V_{\mathrm{E}33} \end{bmatrix} \tag{11}$$

with:

$$V_{\mathrm{E}11} = -\rho U_{\mathrm{C}1} + \rho\sqrt{3}U_{\mathrm{C}5} + V_{zz}(0)(\eta_0 - 1)/2$$

$$V_{\mathrm{E}22} = -\rho U_{\mathrm{C}1} - \rho\sqrt{3}U_{\mathrm{C}5} - V_{zz}(0)(\eta_0 + 1)/2$$

$$V_{\mathrm{E}33} = 2\rho U_{\mathrm{C}1} + V_{zz}(0).$$

The random components $U_{\mathrm{E}k}$ $(k = 1, \ldots, 5)$ of the vector $\boldsymbol{U}_{\mathrm{E}} = \boldsymbol{U}(0) + \rho\boldsymbol{U}_{\mathrm{C}}$ associated with $\bar{\boldsymbol{V}}_{\mathrm{E}}(\varepsilon)$ are then independent Gaussian random variables with variances ρ^2 and means $\boldsymbol{\mu} = \langle \boldsymbol{U}(0) \rangle$.

3.3. The distribution of the norm of the sum tensor

We derive in this section the distribution of the norm of $\bar{\boldsymbol{V}}_{\mathrm{E}}(\varepsilon)$ and we describe exact characteristics of it which are of practical interest for the extended model (section 4.1). The mean of the square of the norm of $\bar{\boldsymbol{V}}_{\mathrm{E}}(\varepsilon)$ is

$$M_\varepsilon^2 = \langle \operatorname{tr} \bar{\boldsymbol{V}}_{\mathrm{E}}^2(\varepsilon) \rangle = M_0^2(1 + \varepsilon^2). \tag{12}$$

The ratio $\frac{M_{\mathrm{RN}}^2}{M_\varepsilon^2}$ is then simply $\frac{\varepsilon^2}{1+\varepsilon^2}$. The distribution of $t = \operatorname{tr} \bar{\boldsymbol{V}}_{\mathrm{E}}^2(\varepsilon)/6\rho^2$ is that of the sum of the squares of five independent Gaussian variables with unit variances and non-zero means. The distribution of $y = \sqrt{t}$ is then a non-central chi distribution with five degrees of freedom [27] and a non-centrality parameter λ^2 which is calculated from the means μ_k and the variances ρ^2 of the $U_{\mathrm{E}k}$s as

$$\lambda^2 = \frac{1}{\rho^2}\sum_{k=1}^{5}\mu_k^2 = \frac{V_{zz}^2(0)(1 + \eta_0^2/3)}{4\rho^2} = \frac{5}{\varepsilon^2}. \tag{13}$$

The density probability of $z = \|\bar{\boldsymbol{V}}_{\mathrm{E}}(\varepsilon)\| = \sqrt{\operatorname{tr}(\bar{\boldsymbol{V}}_{\mathrm{E}}^2(\varepsilon))}$ is finally deduced from that classical distribution to be

$$p(z) = \sqrt{\frac{2}{\pi}}\frac{z}{\lambda M_0^2}\exp\left(-\frac{\lambda^2}{2}\left(1 + \frac{z^2}{M_0^2}\right)\right) \times \left\{\frac{\lambda^2 z}{M_0}\cosh\left(\frac{\lambda^2 z}{M_0}\right) - \sinh\left(\frac{\lambda^2 z}{M_0}\right)\right\} \qquad z > 0. \tag{14}$$

The functional form given by equation (14) is that which would be observed by Mössbauer spectroscopy for the quadrupole splitting distribution of a disordered solid modelled by equation (8) in a non-magnetic state. Equation (14) still holds, with the appropriate λ (equation (13)), when all components of $\boldsymbol{U}_{\mathrm{E}}$, and not only $U_{\mathrm{E}1}$ and $U_{\mathrm{E}5}$, have non-zero means. The mean $\langle z \rangle = \langle |V_{zz}|\sqrt{1 + \eta^2/3} \rangle$ and the ratio $r_\Delta(\varepsilon) = \frac{\sigma(|V_{zz}|\sqrt{1+\eta^2/3})}{\langle z \rangle}$, with $\sigma^2(|V_{zz}|\sqrt{1 + \eta^2/3}) = \langle (|V_{zz}|\sqrt{1 + \eta^2/3} - \langle z \rangle)^2 \rangle$, are finally given by

$$\langle z \rangle = M_0\tau(\varepsilon)$$

$$\tau(\varepsilon) = \frac{1}{25}\left\{\sqrt{\frac{10}{\pi}}\varepsilon(5 + \varepsilon^2)\exp\left(-\frac{5}{2\varepsilon^2}\right) + (25 + 10\varepsilon^2 - \varepsilon^4)\operatorname{erf}\left(\frac{1}{\varepsilon}\sqrt{\frac{5}{2}}\right)\right\} \tag{15}$$

$$r_\Delta(\varepsilon) = \sqrt{\frac{1 + \varepsilon^2}{\tau(\varepsilon)^2} - 1},$$

where $\operatorname{erf}(x)$ is the error function ($\operatorname{erf}(x) = \frac{2}{\sqrt{\pi}}\int_0^x \exp(-t^2)\,\mathrm{d}t$). When $\varepsilon \to 0$, the four first terms of the expansion of $\tau(\varepsilon)$ are $1 + \frac{2\varepsilon^2}{15} - \frac{\varepsilon^4}{25} + \frac{8}{125}\sqrt{\frac{2}{5\pi}}\varepsilon^7$. The asymptotic value of $r_\Delta(\varepsilon)$ is that of the Czjzek model, $r_\Delta(\infty) = \sqrt{\frac{45\pi}{128} - 1} = 0.323\,212\ldots$. The mean norm of $\bar{\boldsymbol{V}}_{\mathrm{E}}(\varepsilon)$ is the product of the norm of the fixed tensor $\bar{\boldsymbol{V}}(0)$ by a function of ε. Thus, the ratio $r_\Delta(\varepsilon)$ is solely determined by ε and is independent of η_0.

3.4. The bivariate distribution $f_{\mathrm{E}}(V_{zz}, \eta)$

For simplicity, the dependence of f_{E} on ε and η_0 is implicit in the notation. The calculation of the bivariate distribution $f_{\mathrm{E}}(V_{zz}, \eta)$ is much more involved than in the Czjzek case and a simple closed form expression like that of equation (4) has not been found. The method of appendix C of [7], starts with the distribution of $\boldsymbol{U}_{\mathrm{E}}$ as obtained from the sum tensor (equations (8)). It gives

$$p(\boldsymbol{U}_{\mathrm{E}}) = \frac{1}{(2\pi\rho^2)^{5/2}}\exp\left(-\frac{M_0^2}{12\rho^2}\right)\exp\left(-\frac{\sum_{k=1}^{5}U_{\mathrm{E}k}^2}{2\rho^2}\right) \times \exp\left(\frac{\vec{U}_{\mathrm{E}}\cdot\vec{\mu}}{\rho^2}\right). \tag{16}$$

To calculate the bivariate distribution $f_{\mathrm{E}}(V_{zz}, \eta)$, it is necessary to diagonalize $\bar{\boldsymbol{V}}_{\mathrm{E}}(\varepsilon)$, that is to change the set of random variables from $\boldsymbol{U}_{\mathrm{E}}$ to $(V_{zz}, \eta, \alpha, \beta, \gamma)$, where (α, β, γ) are Euler angles $(0 \leqslant \alpha < 2\pi, 0 \leqslant \beta < \pi, 0 \leqslant \gamma < 2\pi)$. First, this introduces the Jacobian of the transformation $\propto \sin(\beta)V_{zz}^4\eta(1 - \frac{\eta^2}{9})$. Then, the components μ_1 and μ_5 must be expressed in a new frame of reference in which the sum tensor is diagonal ($U_{\mathrm{E}1} = V_{zz}/2, U_{\mathrm{E}2} = U_{\mathrm{E}3} = U_{\mathrm{E}4} = 0, U_{\mathrm{E}5} = \eta V_{zz}/2\sqrt{3}$). The distribution $p_{\mathrm{E}}(\boldsymbol{D})$ which is obtained in that way, where $\boldsymbol{D} = (V_{zz}, \eta, t = 2\alpha, u = \cos\beta, v = 2\gamma)$, needs to be integrated $(0 \leqslant t \leqslant 2\pi, -1 \leqslant u \leqslant 1, 0 \leqslant v \leqslant 2\pi)$ to yield $f_{\mathrm{E}}(V_{zz}, \eta)$. The latter step seems however intractable. The case $\eta_0 = 0$ is somewhat simpler and reduces to [7]

$$f_{\mathrm{E}}(V_{zz}, \eta) \propto \eta\left(1 - \frac{\eta^2}{9}\right)V_{zz}^4 \times \exp\left(-\frac{(V_{zz}^2(0) + V_{zz}^2(1 + \eta^2/3))}{8\rho^2}\right) \times \int_0^1 \exp(\Phi(3u^2 - 1))I_0(\eta|\Phi|(1 - u^2))\,\mathrm{d}u, \tag{17}$$

where $I_0(x)$ is a modified Bessel function of the first kind and $\Phi = V_{zz}V_{zz}(0)/8\rho^2$. Equation (17) yields the expected equation (4) for $V_{zz}(0) = 0$ and $\rho = \sigma_{\mathrm{C}}/2$ (the factor $1/2$ comes from the specific choice of the $\bar{\boldsymbol{V}}_{\mathrm{C}}$ tensor in equation (8)). As the equation which expresses $f_{\mathrm{E}}(V_{zz}, \eta)$ is difficult to handle, we resorted to Monte Carlo simulations of equation (8), as described in section 4, to get the overall evolution of both $f_{\mathrm{E}}(V_{zz}, \eta)$ and $p_{\mathrm{E}}(V_{zz}, \eta) = 2f_{\mathrm{E}}(V_{zz}, \eta)(V_{zz} \geqslant 0, 0 \leqslant \eta \leqslant 1)$ as a function of η_0 and ε (figures 12–17 of section 4 for $\eta_0 = 0.3$). The random variables V_{zz} and η are dependent as they are for the Czjzek model.

Table 1. Comparison of simulated (10^8 tensors) and theoretical means and standard-deviations for the Czjzek model with $\sigma_C = 1$.

Means and standard-deviations	Simulated values	Theoretical values
$\langle\eta\rangle_C$	0.609 81	0.609 823 . . .
$\sigma_{\eta,C}$	0.242 69	0.242 685 . . .
$\langle\|V_{zz}\|\rangle_C$	3.989 42	3.989 422 . . .
$\sigma_{\|V_{zz}\|,C}$	1.300 81	1.300 846 . . .

3.5. Small perturbations

Using perturbation theory, for instance lemma 2.1 of [28], the principal values of $\bar{\boldsymbol{V}}_{\rm E}(\varepsilon)$ (equation (8)), which is a diagonal tensor $\bar{\boldsymbol{V}}(0)$, whose principal values are all assumed to be different ($\eta_0 \neq 0$), perturbed by a symmetric tensor $\rho\bar{\boldsymbol{V}}_{\rm C}$ are just the diagonal elements of the tensor $\bar{\boldsymbol{V}}_{\rm E}(\varepsilon)$ from which we write

$$\begin{aligned} v_{xx}(\varepsilon) - v_{yy}(\varepsilon) &= \eta_0 V_{zz}(0) + 2\rho\sqrt{3}U_{c5} + o(\varepsilon) \\ v_{zz}(\varepsilon) &= V_{zz}(0) - 2\rho U_{c1} + o(\varepsilon), \end{aligned} \tag{18}$$

where the unsorted principal values are denoted by lower case symbols. The asymmetry parameter expanded for very small values of $\rho/V_{zz}(0)$ gives

$$\eta(\varepsilon) \approx \eta_0 + \frac{2\rho}{V_{zz}(0)}(\sqrt{3}U_{C5} + \eta_0 U_{C1}) + O(\rho^2). \tag{19}$$

The distribution of $\eta(\varepsilon)$ is then Gaussian with a mean η_0 and a standard-deviation $\varepsilon\sqrt{\frac{3}{5}(1+\frac{\eta_0^2}{3})}$. The latter conclusions actually hold only when η_0 ranges between ∼0.2 and ∼0.8 with $\varepsilon \leqslant$ ∼0.04–0.05. We will show in the next section that the distribution of η is indeed Gaussian in a broad range of η_0 when ε is small (figure 7). The broadening, which increases when η_0 increases, would depend identically on η_0 when choosing $|V_{zz}(0)|\sqrt{(1+\eta_0^2/3)} = 1$ instead of $|V_{zz}(0)| = 1$. It is clearly seen in figure 7 for $\varepsilon = 0.05$. When $\eta_0 = 0$, a small perturbation on the EFG tensor only slightly changes the magnitudes of the principal components but it suffices to change significantly the asymmetry parameter, because the latter is a ratio. The consequence is a zero probability for $\eta = 0$, even for very small values of ε, a result which holds for any η_0 (section 4.2).

4. Monte Carlo simulations

The distributions of all parameters were obtained with high precision in the whole range of η_0 and ε by direct Monte Carlo simulations of equation (8) with a Fortran code running on a standard laptop computer. Gaussian random variables were generated by the classical Box–Müller method [18]. For that purpose, two independent random numbers, x_1 and x_2, uniformly distributed between 0 and 1, are first generated. Then, the following variables, $y_1 = \sigma_1\sqrt{-2\ln(x_1)}\sin(2\pi x_2) + m_1$ and $y_2 = \sigma_2\sqrt{-2\ln(x_1)}\cos(2\pi x_2) + m_2$ are two independent Gaussian variables with standard-deviations σ_1 and σ_2 and means m_1 and m_2 respectively. The considered distributions and their moments were calculated from $N = 25 \times 10^6$ up to $N = 10^8$ simulated tensors. The value of $V_{zz}(0)$ was set to 1 without loss of generality. Another choice might have been to set $V_{zz}(0)\sqrt{1+\eta_0^2/3} = 1$. A direct simulation of the Czjzek model with $\sigma_{\rm C} = 1$ yields the simulated values ($N = 10^8$) given in table 1. They are in excellent agreement with the theoretical values, with absolute values of deviations being typically less than 10^{-4}.

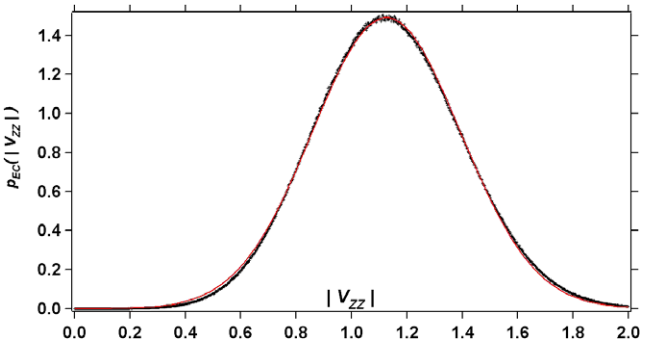

Figure 1. Distribution $p_{\rm E}(|V_{zz}|)$ of the absolute value of V_{zz} for $\eta_0 = 0.5$ and $\varepsilon = 0.64$ (solid line = Gaussian).

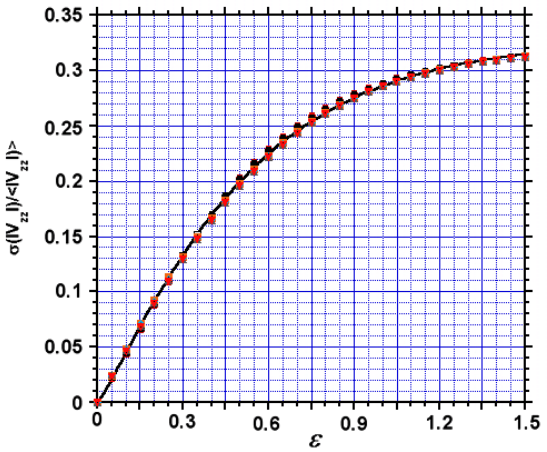

Figure 2. Variation with ε of the ratio $r_{\eta_0}(\varepsilon) = \sigma(|V_{zz}|)/\langle|V_{zz}|\rangle$.

4.1. The distribution $p_{\rm E}(v)$

The distribution $p_{\rm E}(v)$ of the absolute value v of V_{zz} is very well approximated by a Gaussian in the whole range of η_0 and of ε investigated here (figure 1). To characterize it, figure 2 shows the ratio $r_{\eta_0}(\varepsilon)$ of the standard-deviation $\sigma_{|V_{zz}|,{\rm E}} = \sqrt{\langle|V_{zz}|^2\rangle_{\rm E} - \langle|V_{zz}|\rangle_{\rm E}^2}$ to the average $\langle|V_{zz}|\rangle_{\rm E}$ as a function of ε for $0 \leqslant \eta_0 \leqslant 1$. The ratio $r_\Delta(\varepsilon)$ (equations (15)), independent of η_0, and the ratio $r_{\eta_0}(\varepsilon)$ would be strictly equal if V_{zz} and η were independent. It is thus not surprising to find that $r_{\eta_0}(\varepsilon)$ is only weakly dependent on η_0. Plots of $r_\Delta(\varepsilon)$ and of $r_{\eta_0}(\varepsilon)$ indeed show that they actually differ by just a little. The complicated expression of $r_\Delta(\varepsilon)$ (equations (15)) makes it obvious that it is hopeless to guess its exact expression or

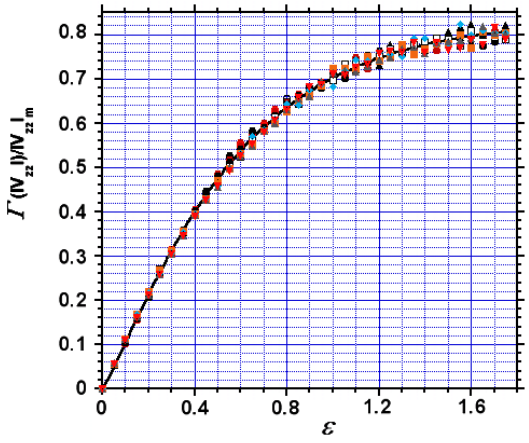

Figure 3. Variation with ε of the ratio $\Gamma_{\eta_0}(\varepsilon) = \Gamma(|V_{zz}|)/|V_{zz}|_m$.

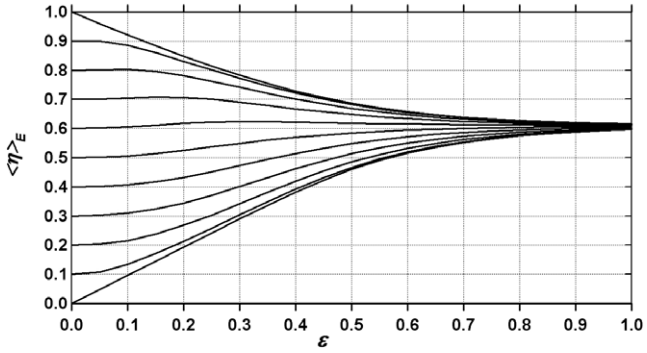

Figure 4. Variation with ε of the mean asymmetry parameter $\langle\eta\rangle_{\rm E}$ for a given value of η_0, which increases by steps of 0.1 from 0 to 1 from bottom to top.

that of $r_{\eta_0}(\varepsilon)$ from Monte Carlo results. We must then rely on a good quality approximation to describe the latter ratio. The solid line in figure 2 interpolates between the values of the average ratio $\bar{r}(\varepsilon) = \sum_{k=0}^{10} r_{\eta_0=0.1k}(\varepsilon)/11$. Neglecting the small dispersion of $r_{\eta_0}(\varepsilon)$ with η_0, we summarize the results of figure 2 by a single good quality approximation:

$$r_{\eta_0}(\varepsilon) = r(\varepsilon) = 0.326\,07(1 - \exp(-2.097\varepsilon^{1.151})), \qquad (20)$$

where the constant 0.326 07 is that of Czjzek's model, $r(\infty)$ (section 2). A fit of the exact $r_\Delta(\varepsilon)$, given by equations (15), by a form similar to that of equation (20) gives $r_{\Delta\rm app}(\varepsilon) = 0.323\,212(1 - \exp(-2.056\,36\varepsilon^{1.156\,81}))$ with $|r_\Delta(\varepsilon) - r_{\Delta\rm app}(\varepsilon)| < 2.5 \times 10^{-3}$ for any ε. It strengthens the confidence in the approximate expressions used here. A simple way to obtain an approximate value of $|V_{zz}(0)|$, when $\langle|V_{zz}|\rangle$ and ε have been determined from experiment and when a value of η_0 has been selected, is just to write from equations (15) that $|V_{zz}(0)| \approx \langle|V_{zz}|\rangle\sqrt{1 + \langle\eta\rangle^2/3}/[\tau(\varepsilon)\sqrt{1 + \eta_0^2/3}]$.

For practical purposes, the ratio $\Gamma_{\eta_0}(\varepsilon)$ of the full width at half maximum (FWHM) of the probability density $p_{\rm E}(v)$ to the position of its maximum $v_{\max}$ was similarly characterized (figure 3). Figure 3 shows again that $\Gamma_{\eta_0}(\varepsilon)$ is almost independent of η_0, as expected from the similar behaviour of $r_{\eta_0}(\varepsilon)$. The dispersion of the ratio around the mean ratio

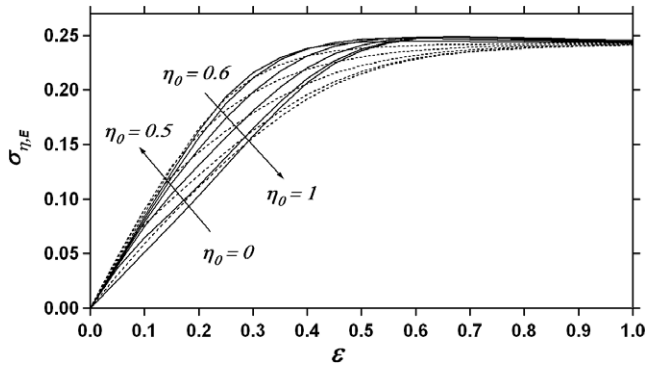

Figure 5. Variation with ε of the standard-deviation $\sigma_{\eta,\rm E}$ for a given value of η_0, which increases by steps of 0.1 from 0 to 1, as indicated by arrows (solid lines from 0 to 0.5, dotted lines from 0.6 to 1).

$\bar{\Gamma}(\varepsilon) = \sum_{k=0}^{10} \Gamma_{\eta_0=0.1k}(\varepsilon)/11$ is larger for $\Gamma_{\eta_0}(\varepsilon)$ than it is for $r_{\eta_0}(\varepsilon)$, in particular for large values of ε. The relevant dispersion is that of figure 2, as $r_{\eta_0}(\varepsilon)$ is calculated directly from the whole set of simulated values while $\Gamma_{\eta_0}(\varepsilon)$ is less precisely evaluated from the maxima and the FWHM's of histograms of $p_{\rm EC}(v)$ built from the simulated values. Again, all the previous results are nicely represented by the relation:

$$\Gamma_{\eta_0}(\varepsilon) = \Gamma(\varepsilon) = 0.831\,25(1 - \exp(-1.862\varepsilon^{1.143})), \qquad (21)$$

where the unpublished value for Czjzek's model is $\Gamma(\infty) = 0.831\,25\ldots$ (section 2.2). For $\varepsilon \leqslant 0.4$, $\Gamma(\varepsilon)$ is fairly well approximated by ε. A Gaussian shape with a maximum at the same position as that of the Czjzek distribution $p_{\rm C}(v)$ (equation (7)), namely $3.734\,206\,82\ldots$ for $\sigma_{\rm C} = 1$ (section 2), and with the same standard-deviation as that of $p_{\rm C}(v)$, $\sigma_{|V_{zz}|} = 1.300\,846\ldots$, would have a ratio Γ_G of 0.820 324, close to 0.831 25. The latter result is fully consistent with the approximate Gaussian shape of $p_{\rm E}(v)$ mentioned above (figure 1). Detailed tables giving the values of the ratios $r_{\eta_0}(\varepsilon)$ and $\Gamma_{\eta_0}(\varepsilon)$ and those of the average, $\langle\eta\rangle_{\rm E}$ (figure 4) and of the standard-deviation $\sigma_{\eta,\rm E} = \sqrt{\langle\eta^2\rangle_{\rm E} - \langle\eta\rangle_{\rm E}^2}$ (figure 5), for $\eta_0 = 0.1k$ ($k = 0, 1, \ldots, 10$) and for $\varepsilon = 0.05m$ ($m = 1, 2, \ldots, 34$), are available on request (GLC). For completeness, we show in figure 6 the variation with ε of the fraction of nuclei whose V_{zz} is of the same sign as $V_{zz}(0)$, which may be of interest for Mössbauer spectroscopy in applied magnetic fields. That fraction shows a rather slow overall decrease towards its limiting value of 0.5 (figure 6).

4.2. The distribution $p_{\rm E}(\eta)$ and its approximation $p_{\rm EA}(\eta)$

The mean asymmetry parameter $\langle\eta\rangle_{\rm E}$ and the standard-deviation $\sigma_{\eta,\rm E}$ are shown in figures 4 and 5 as a function of ε for fixed values of η_0. Both characteristics tend rather rapidly to the corresponding values of the Czjzek model ($\varepsilon \to \infty$). The values reached at $\varepsilon = 1$ are already close to their asymptotic values. The distribution $p_{\rm E}(\eta)$, which would be deduced from equations (18), is obtained here from numerical simulations. For small enough ε, and for η_0 not too close to 0 or to 1, the distribution $p_{\rm E}(\eta)$ is essentially a Gaussian (figure 7), fully determined by $\langle\eta\rangle_{\rm E}$ and by $\sigma_{\eta,\rm E}$ (figures 4

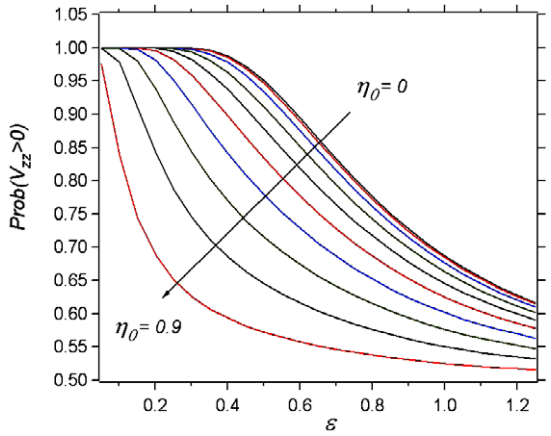

Figure 6. Variation with ε of the probability that V_{zz} has the same sign as $V_{zz}(0)$ (chosen here as positive) for a given value of η_0, which increases by steps of 0.1 from 0 to 0.9, as indicated by the arrow.

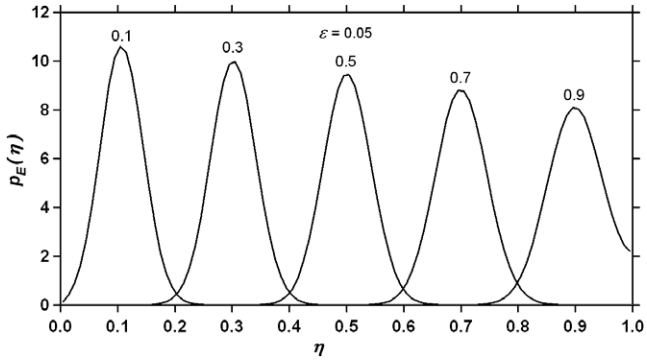

Figure 7. Distributions $p_{\mathrm{E}}(\eta)$ of the asymmetry parameter for $\varepsilon = 0.05$ and $\eta_0 = 0.1, 0.3, 0.5, 0.7, 0.9$.

and 5). For small values of ε, both $p_{\mathrm{E}}(\eta)$ and $p_{\mathrm{E}}(|V_{zz}|)$ are then Gaussians. Rather small perturbations of a well-defined neighbourhood by a Czjzek noise thus provide examples of the simultaneous occurrence of Gaussian distributions of η and $|V_{zz}|$, an assumption (empirical in many cases) which was and is often used to account for NMR lineshapes (section 5). The distributions spread out progressively in the full range of η when ε increases (figures 7–11). This spreading is constrained by the fact that $p_{\mathrm{E}}(0) = 0$ for any η_0 (figures 7–11). This is due to the basic similarity between the zero probability of finding an EFG with $\eta = 0$, and the level-repulsion found in random-matrix theory, as both originate from geometrical correlations due to the Jacobian (section 3.4 and [7]). That constraint produces an overall asymmetry of the distribution $p_{\mathrm{E}}(\eta)$, as it exhibits a rather rapidly increasing contribution around $\eta = 1$. That asymmetry is the weakest for central values of η_0 and for small values of ε (figure 7).

The distribution $p_{\mathrm{E}}(\eta)$ is observed to be very well approximated by the distribution $p_{\mathrm{EA}}(\eta)$, given below for the whole range of variation of η_0 and of ε (figures 7–11):

$$0 \leqslant \eta \leqslant 1$$

$$p_{\mathrm{EA}}(\eta) = \frac{\beta k^{((1+\alpha)/\beta)}}{\Gamma\left(\frac{1+\alpha}{\beta}\right)}[\eta^{\alpha}\exp(-k\eta^{\beta}) + (2-\eta)^{\alpha} \times \exp(-k(2-\eta)^{\beta})]. \quad (22)$$

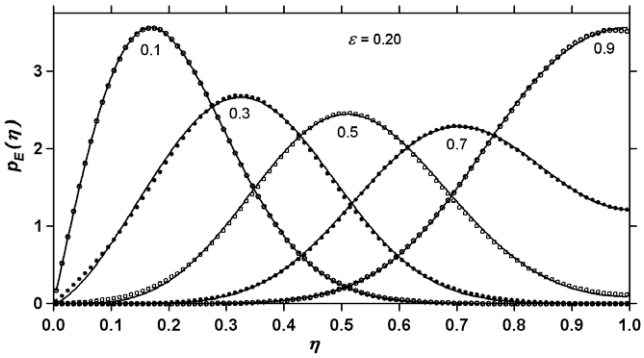

Figure 8. Distributions $p_{\mathrm{E}}(\eta)$ of the asymmetry parameter for $\varepsilon = 0.20$ and $\eta_0 = 0.1, 0.3, 0.5, 0.7, 0.9$ (empty and solid symbols) and their approximations (solid lines) by $p_{\mathrm{EA}}(\eta)$ (equation (22)).

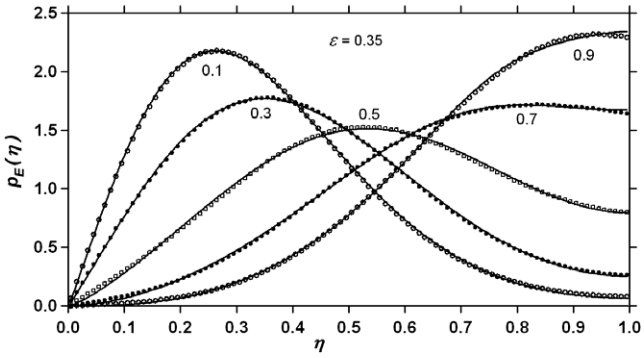

Figure 9. Distributions $p_{\mathrm{E}}(\eta)$ of the asymmetry parameter for $\varepsilon = 0.35$ and $\eta_0 = 0.1, 0.3, 0.5, 0.7, 0.9$ (empty and solid symbols) and their approximations (solid lines) by $p_{\mathrm{EA}}(\eta)$ (equation (22)).

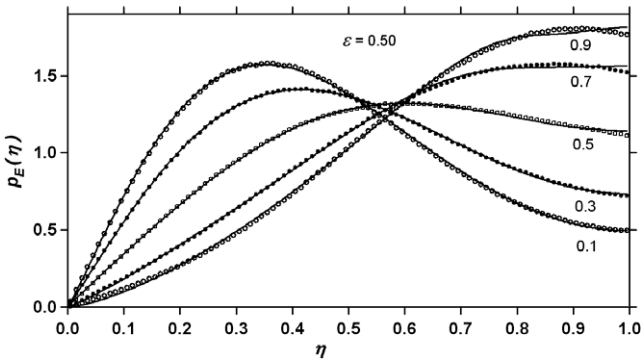

Figure 10. Distributions $p_{\mathrm{E}}(\eta)$ of the asymmetry parameter for $\varepsilon = 0.50$ and $\eta_0 = 0.1, 0.3, 0.5, 0.7, 0.9$ (empty and solid symbols) and their approximations (solid lines) by $p_{\mathrm{EA}}(\eta)$ (equation (22)).

The various terms were chosen as follows: the η^{α} term ensures that $p_{\mathrm{EA}}(0) = 0$ for any η_0 and $\varepsilon(>0)$, the exponential term yields a Gaussian shape for $\varepsilon \to 0$, while the second term gives the correct behaviour for $\eta \sim 1$ together with a negligible contribution at $\eta = 0$. The three parameters k, α and β were determined and are tabulated as a function of η_0 and ε (table 2). The probability density of a generalized gamma

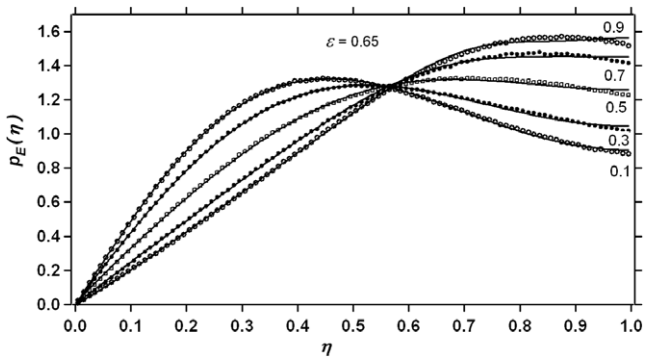

Figure 11. Distributions $p_{\mathrm{E}}(\eta)$ of the asymmetry parameter for $\varepsilon = 0.65$ and $\eta_0 = 0.1, 0.3, 0.5, 0.7, 0.9$ (empty and solid symbols) and their approximations (solid lines) by $p_{\mathrm{EA}}(\eta)$ (equations (22)).

distribution [29] is written as

$$p(x) = \frac{\beta k^{(1+\alpha)/\beta}}{\Gamma((1+\alpha)/\beta)} x^{\alpha} \exp(-kx^{\beta}) \qquad x > 0 \qquad (23)$$

where $\Gamma(x)$ is the Euler gamma function ($\Gamma(x) = \int_0^{\infty} y^{x-1} \mathrm{e}^{-y}\, \mathrm{d}y$). Its moments are

$$\langle x^n \rangle = \frac{\Gamma((1+n+\alpha)/\beta)}{k^{n/\beta}\Gamma((1+\alpha)/\beta)}. \qquad (24)$$

The normalizing coefficient of equations (22), which comes from equation (23), is only strictly valid for an unconstrained range of η, but the integral of $\int_0^1 p_{\mathrm{EA}}(\eta)\, \mathrm{d}\eta$ in practice deviates negligibly from 1. The largest deviation from 1 is at most of the order of some 10^{-4}. The distribution equation (22) is even a very good approximation of the Czjzek distribution $p_{\mathrm{C}}(\eta)$ (equation (5)) with $k_\infty = 1.346, \alpha_\infty = 0.930, \beta_\infty = 3.348$. The mean asymmetry parameter $\langle\eta\rangle_\infty$ and the standard-deviation $\sigma_{\eta,\infty}$ obtained from that approximation are 0.609 75 and 0.2431 respectively while they are 0.609 82 and 0.242 68 for $p_{\mathrm{C}}(\eta)$.

When ε decreases down to 0, α increases (table 2). It becomes so large for small values of ε that it cannot be determined properly in most cases. This is the reason why it is not given for very small values of ε in table 2. When α becomes very large for small enough ε and for η_0 not too close to 0 or to 1, the distribution $p_{\mathrm{EA}}(\eta)$ reduces essentially to a Gaussian determined by $\langle\eta\rangle_{\mathrm{E}}$ and by $\sigma_{\eta,\mathrm{E}}$, as described above. The parameter α is of the order of 1 for large values of ε.

The various characteristics of the bivariate distribution $p_{\mathrm{E}}(V_{zz}, \eta)$ have been seen to converge at different 'speeds' towards those of the Czjzek's model. Examples of such bivariate distributions, obtained by Monte Carlo simulations, are shown for $\eta_0 = 0.3$ and for different values of ε in figures 12–17. The asymmetry parameter distribution is close to $p_{\mathrm{C}}(\eta)$ for $\varepsilon \approx 1$ for any η_0.

Section 5 describes a simple trial and error method to find the parameters of the extended Czjzek model and compares some NMR spectra of glasses with the model ones.

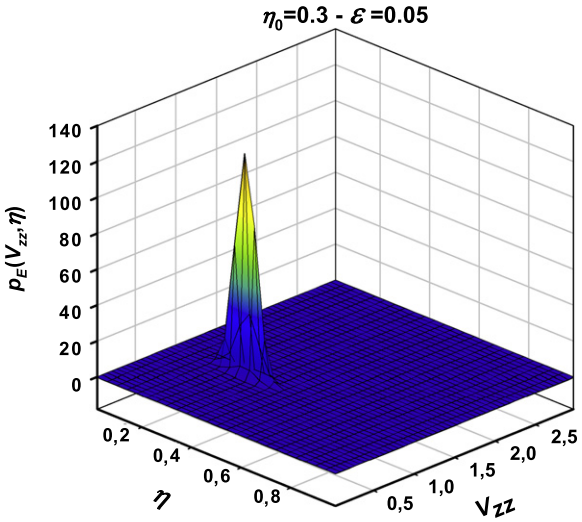

Figure 12. Bivariate distribution $p_{\mathrm{E}}(V_{zz}, \eta)$ for $\eta_0 = 0.3$ and for $\varepsilon = 0.05$.

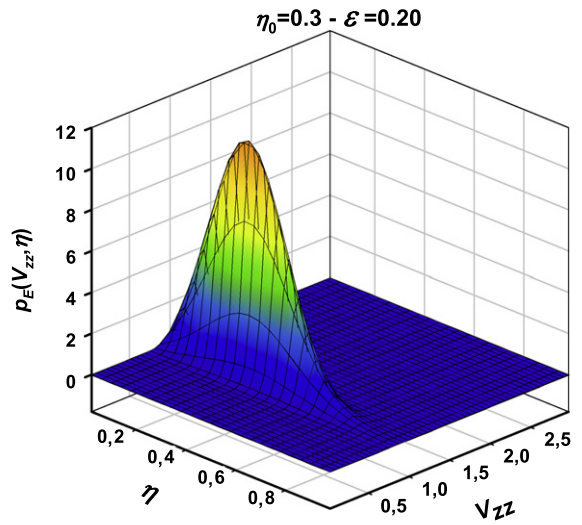

Figure 13. Bivariate distribution $p_{\mathrm{E}}(V_{zz}, \eta)$ for $\eta_0 = 0.3$ and for $\varepsilon = 0.20$.

5. Application to NMR spectra of glasses

The NMR lines of quadrupolar nuclei in disordered solids often exhibit an asymmetric shape tailing towards the high-field side [3, 30–41]. Independent Gaussian distributions of $\nu_Q = \frac{3|eQV_{zz}|}{2I(2I-1)}$ and of η are often assumed to reconstruct the line shape in the static or in the magic angle spinning mode (similar methods are used in EPR (see for instance [42])). This method is convenient to obtain the relative intensity of each contribution, but its physical basis remains to be justified for the specific materials under investigation. Often, the Czjzek model accounts better for the experimental spectra than the Gaussian approximation [3, 31–33, 39, 42–45] while being based on the two clear assumptions whose generality was discussed previously. Their relevance can be made plausible, or even be proven from theoretical calculations, for the considered solids. As advocated in [3], the latter model is

Table 2. The marginal distribution $p_{\mathrm{E}}(\eta)$ of the extended Czjzek model is very well approximated by the distribution $p_{\mathrm{EA}}(\eta)$ (equation (22)) for any pair of values (η_0, ε). The three parameters k, α and β are tabulated below for $\eta_0 = 0.1k$ ($k = 0, 1, \ldots, 10$) and for $\varepsilon = 0.05m$ ($m = 1, 2, \ldots, 22$) ($k_\infty = 1.346$, $\alpha_\infty = 0.930$, $\beta_\infty = 3.338$).

ε	k	α	β	ε	k	α	β	ε	k	α	β	ε	k	α	β
	$\eta_0 = 0$				$\eta_0 = 0.1$				$\eta_0 = 0.2$				$\eta_0 = 0.3$		
0.05	322.000	1.001	1.988	0.05	—	—-	—	0.05	—	—	—	0.05	—	—	—
0.10	79.868	1.006	1.971	0.10	—	—	—	0.10	—	—	—	0.10	—	—	—
0.15	34.827	1.013	1.939	0.15	29.620	0.995	2.103	0.15	31.089	1.269	2.820	0.15	22.689	2.405	2.867
0.20	19.381	1.024	1.895	0.20	16.725	1.013	1.953	0.20	14.422	1.043	2.400	0.20	12.085	1.481	2.774
0.25	12.421	1.037	1.843	0.25	11.147	1.030	1.870	0.25	9.073	1.015	2.108	0.25	7.397	1.166	2.494
0.30	8.763	1.049	1.789	0.30	8.089	1.046	1.800	0.30	6.680	1.036	1.913	0.30	5.309	1.084	2.179
0.35	6.632	1.076	1.712	0.35	6.255	1.076	1.714	0.35	5.342	1.064	1.780	0.35	4.287	1.060	1.977
0.40	5.319	1.098	1.643	0.40	5.086	1.096	1.648	0.40	4.470	1.079	1.700	0.40	3.660	1.053	1.856
0.45	4.431	1.102	1.604	0.45	4.269	1.097	1.614	0.45	3.830	1.079	1.661	0.45	3.209	1.048	1.789
0.50	3.783	1.094	1.594	0.50	3.665	1.089	1.606	0.50	3.336	1.070	1.652	0.50	2.852	1.040	1.765
0.55	3.274	1.076	1.612	0.55	3.186	1.071	1.624	0.55	2.932	1.054	1.671	0.55	2.550	1.026	1.784
0.60	2.870	1.056	1.647	0.60	2.802	1.051	1.662	0.60	2.601	1.036	1.716	0.60	2.290	1.006	1.843
0.65	2.550	1.037	1.704	0.65	2.496	1.033	1.721	0.65	2.334	1.018	1.783	0.65	2.087	0.993	1.916
0.70	2.277	1.013	1.793	0.70	2.224	1.005	1.825	0.70	2.088	0.988	1.908	0.70	1.893	0.966	2.063
0.75	2.053	0.989	1.909	0.75	2.014	0.984	1.941	0.75	1.912	0.971	2.026	0.75	1.766	0.956	2.180
0.80	1.882	0.970	2.041	0.80	1.854	0.966	2.070	0.80	1.776	0.957	2.159	0.80	1.664	0.945	2.318
0.85	1.749	0.953	2.186	0.85	1.730	0.951	2.210	0.85	1.671	0.945	2.294	0.85	1.587	0.937	2.447
0.90	1.656	0.945	2.316	0.90	1.644	0.946	2.331	0.90	1.601	0.942	2.407	0.90	1.537	0.936	2.550
0.95	1.586	0.939	2.432	0.95	1.575	0.939	2.454	0.95	1.545	0.938	2.520	0.95	1.497	0.935	2.648
1.00	1.525	0.932	2.589	1.00	1.516	0.931	2.616	1.00	1.489	0.928	2.696	1.00	1.452	0.926	2.817
1.05	1.494	0.933	2.658	1.05	1.485	0.932	2.689	1.05	1.462	0.929	2.770	1.05	1.432	0.927	2.887
1.10	1.459	0.929	2.786	1.10	1.452	0.928	2.812	1.10	1.437	0.927	2.874	1.10	1.416	0.928	2.962
	$\eta_0 = 0.4$				$\eta_0 = 0.5$				$\eta_0 = 0.6$				$\eta_0 = 0.7$		
0.05	—	—	—	0.05	—	—	—	0.05	—	—	—	0.05	—	—	—
0.10	—	—	—	0.10	—	—	—	0.10	28.740	20.408	2.352	0.10	28.586	28.412	2.125
0.15	17.019	4.132	2.711	0.15	31.904	14.160	2.532	0.15	12.904	9.215	2.334	0.15	12.545	12.495	2.157
0.20	9.425	2.408	2.695	0.20	14.138	6.362	2.542	0.20	7.258	5.218	2.340	0.20	6.375	6.514	2.376
0.25	5.954	1.659	2.582	0.25	7.983	3.711	2.489	0.25	4.407	3.189	2.522	0.25	3.585	3.813	2.788
0.30	4.250	1.304	2.422	0.30	5.083	2.414	2.495	0.30	2.874	2.104	2.850	0.30	2.248	2.488	3.499
0.35	3.359	1.128	2.286	0.35	3.497	1.679	2.599	0.35	2.059	1.526	3.272	0.35	1.626	1.816	4.535
0.40	2.853	1.052	2.157	0.40	2.631	1.292	2.678	0.40	1.651	1.234	3.653	0.40	1.352	1.467	5.542
0.45	2.531	1.021	2.061	0.45	2.168	1.107	2.668	0.45	1.451	1.087	3.910	0.45	1.227	1.265	6.190
0.50	2.289	1.002	2.020	0.50	1.911	1.022	2.615	0.50	1.360	1.012	3.984	0.50	1.174	1.138	6.362
0.55	2.091	0.987	2.033	0.55	1.753	0.979	2.583	0.55	1.321	0.974	3.950	0.55	1.161	1.060	6.075
0.60	1.920	0.970	2.103	0.60	1.644	0.955	2.599	0.60	1.310	0.955	3.821	0.60	1.166	1.008	5.658
0.65	1.790	0.960	2.188	0.65	1.566	0.942	2.651	0.65	1.308	0.943	3.746	0.65	1.185	0.979	5.190
0.70	1.672	0.943	2.340	0.70	1.512	0.936	2.721	0.70	1.314	0.939	3.629	0.70	1.213	0.965	4.667
0.75	1.600	0.940	2.439	0.75	1.467	0.930	2.832	0.75	1.324	0.939	3.517	0.75	1.236	0.953	4.350
0.80	1.538	0.934	2.576	0.80	1.445	0.933	2.874	0.80	1.327	0.937	3.475	0.80	1.260	0.949	4.039
0.85	1.492	0.930	2.686	0.85	1.422	0.931	2.961	0.85	1.329	0.933	3.457	0.85	1.275	0.942	3.895
0.90	1.462	0.931	2.779	0.90	1.403	0.929	3.029	0.90	1.331	0.932	3.433	0.90	1.289	0.939	3.761
0.95	1.439	0.932	2.850	0.95	1.390	0.928	3.088	0.95	1.335	0.933	3.400	0.95	1.298	0.936	3.685
1.00	1.410	0.926	2.986	1.00	1.383	0.930	3.114	1.00	1.332	0.929	3.426	1.00	1.305	0.933	3.614
1.05	1.399	0.927	3.028	1.05	1.368	0.926	3.202	1.05	1.337	0.930	3.379	1.05	1.315	0.933	3.549
1.10	1.390	0.929	3.084	1.10	1.366	0.928	3.198	1.10	1.341	0.932	3.370	1.10	1.323	0.934	3.497

(or might be) useful to reconstruct properly most of individual lines of ^{7}Li, ^{23}Na, ^{27}Al, ^{71}Ga, or of other quadrupolar nuclei, in glasses, especially glasses in which chemical bonds are dominated by ionic interactions, typically oxide and halide glasses. Indeed, ionic bonding is generally associated with higher coordination numbers around the quadrupolar probe with a somewhat more isotropic local arrangement than in covalent materials. D'Espinose de Lacaillerie *et al* review the applications of the Czjzek distribution to solid state NMR [3]. Figure 18 shows the example of a ^{71}Ga spectrum recorded in static mode in a fluoride glass from the pseudo-ternary system PbF_2–ZnF_2–GaF_3 with its reconstruction from a Czjzek distribution [31].

Solid state NMR has been recently applied to the characterization of chalcogenide glasses, namely glasses based on sulfur, selenium or tellurium, for optical applications. Significant structural information was obtained using ^{77}Se as a probe in As_xSe_{1-x}, Ge_xSe_{1-x}, Te_xSe_{1-x} binary glasses [46–49]. Generally speaking, chalcogenide glasses are constituted of elements which are very close to each other in the right part of the periodic chart. The chalcogen atoms are most often associated with germanium, arsenic, antimony, gallium, to name a few. When compared to the structures of oxide glasses, or to those of fluoride glasses, their structural networks are dominated by covalent and directional bonds with low coordination numbers (from 2 to 4) [50, 51].

Table 2. (Continued.)

ε	k	α	β	ε	k	α	β	ε	k	α	β
	$\eta_0 = 0.8$				$\eta_0 = 0.9$				$\eta_0 = 1.0$		
0.05	—	—	—	0.05	—	—	—	0.05	—	—	—
0.10	25.921	34.130	2.115	0.10	13.744	29.682	4.314	0.10	5.344	24.987	7.117
0.15	9.765	13.722	2.379	0.15	4.512	13.946	4.331	0.15	3.906	13.591	5.898
0.20	4.606	7.009	2.900	0.20	2.062	7.203	5.045	0.20	2.746	8.109	6.024
0.25	2.542	4.173	3.898	0.25	2.855	4.812	5.961	0.25	2.112	5.376	6.337
0.30	1.764	2.904	5.207	0.30	2.061	3.496	6.663	0.30	1.720	3.812	6.856
0.35	1.436	2.226	6.416	0.35	1.678	2.660	7.352	0.35	1.476	2.853	7.427
0.40	1.273	1.803	7.352	0.40	1.443	2.107	7.964	0.40	1.319	2.230	7.976
0.45	1.181	1.514	7.954	0.45	1.297	1.723	8.472	0.45	1.213	1.804	8.458
0.50	1.134	1.316	7.997	0.50	1.199	1.459	8.546	0.50	1.146	1.509	8.677
0.55	1.115	1.180	7.642	0.55	1.141	1.273	8.348	0.55	1.110	1.305	8.582
0.60	1.112	1.084	7.158	0.60	1.110	1.145	7.912	0.60	1.098	1.168	8.071
0.65	1.127	1.025	6.489	0.65	1.099	1.066	7.115	0.65	1.107	1.082	7.218
0.70	1.156	0.993	5.661	0.70	1.109	1.015	6.316	0.70	1.123	1.023	6.519
0.75	1.191	0.976	4.964	0.75	1.130	0.988	5.461	0.75	1.155	0.992	5.660
0.80	1.216	0.961	4.556	0.80	1.164	0.969	4.928	0.80	1.182	0.971	5.091
0.85	1.240	0.952	4.270	0.85	1.191	0.949	4.233	0.85	1.214	0.960	4.608
0.90	1.260	0.945	4.042	0.90	1.243	0.949	4.232	0.90	1.237	0.950	4.313
0.95	1.273	0.939	3.915	0.95	1.243	0.942	4.056	0.95	1.255	0.944	4.085
1.00	1.290	0.939	3.734	1.00	1.258	0.943	3.808	1.00	1.278	0.944	3.839
1.05	1.299	0.935	3.684	1.05	1.281	0.937	3.770	1.05	1.288	0.937	3.806
1.10	1.310	0.936	3.596	1.10	1.290	0.937	3.666	1.10	1.298	0.937	3.695

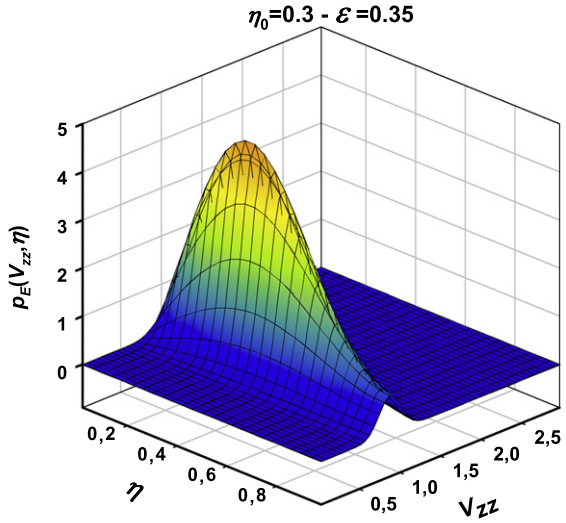

Figure 14. Bivariate distribution $p_{\mathrm{E}}(V_{zz}, \eta)$ for $\eta_0 = 0.3$ and for $\varepsilon = 0.35$.

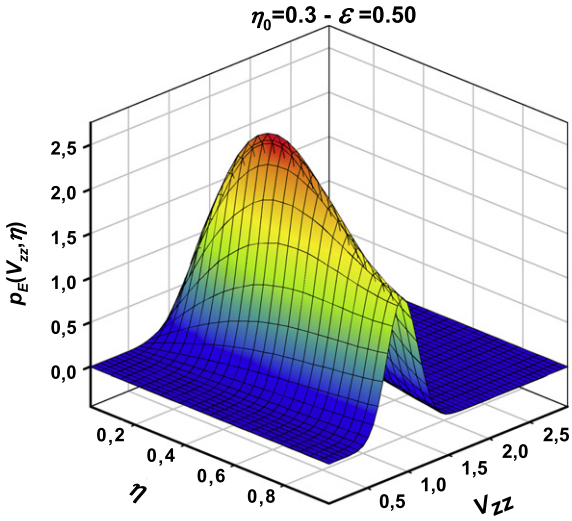

Figure 15. Bivariate distribution $p_{\mathrm{E}}(V_{zz}, \eta)$ for $\eta_0 = 0.3$ and for $\varepsilon = 0.50$.

Unfortunately, only very few NMR nuclei are available to probe their structures. Besides ^{77}Se, whose nuclear quadrupole moment is 0, since $I = 1/2$, almost only the ^{71,69}Ga isotopes are left to perform such studies. Indeed, gallium is usually added to some glass compositions, either for the purpose of being substituted by rare-earth atoms for luminescence or to act as a nucleating agent to prepare glass ceramics [52, 53]. In that context, some ^{71}Ga NMR spectra were collected in glasses, for instance those of the pseudo-ternary system GeS_2–Ga_2S_3–CsCl. The ^{71}Ga (spin $I = 3/2$) spectra were recorded at room temperature on an Avance 300 Bruker spectrometer operating at 91.5 MHz with a static probe. Full echoes were acquired to improve the signal to noise ratio and to avoid any distortion of the baseline. The pulse length, t_{pulse}, was chosen to be much smaller than $t_{\pi/2}$ ($t_{\pi/2} \approx 4t_{\mathrm{pulse}}$) to ensure a linear irradiation regime over the whole frequency range. Due to the strong quadrupolar effect, Magic Angle Spinning techniques did not permit the efficient reduction of the linewidths.

The contribution of the ^{71}Ga NMR to the understanding of the nucleation-growth process in these glass ceramic families will be discussed elsewhere. Here, we focus on the original shape of the gallium line in a 25% GeS_2-75% Ga_2S_3 glass (figure 19). The lineshape, which is due to the quadrupolar effect, is clearly different from that usually observed in oxide or fluoride glasses. Generally speaking, it is the η_Q distribution which determines the shape of the NMR line, whereas the spreading of ν_Q plays a secondary role. The extension of the Czjzek model described in the present paper, allows us

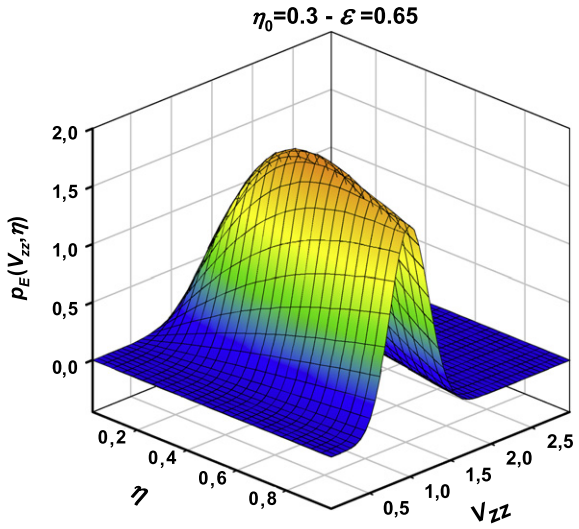

Figure 16. Bivariate distribution $p_{\mathrm{E}}(V_{zz}, \eta)$ for $\eta_0 = 0.3$ and for $\varepsilon = 0.65$.

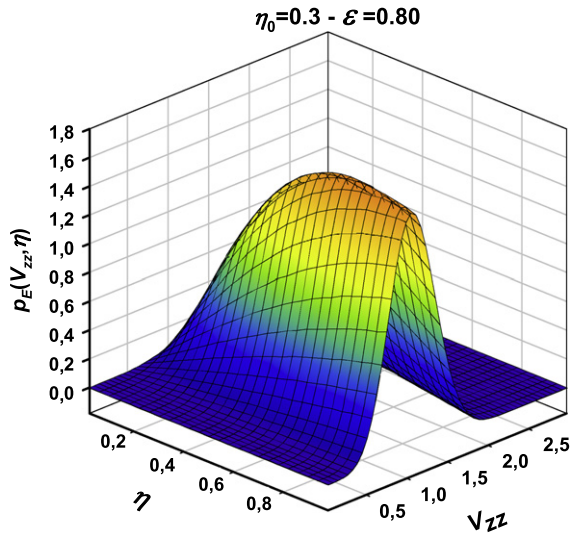

Figure 17. Bivariate distribution $p_{\mathrm{E}}(V_{zz}, \eta)$ for $\eta_0 = 0.3$ and for $\varepsilon = 0.80$.

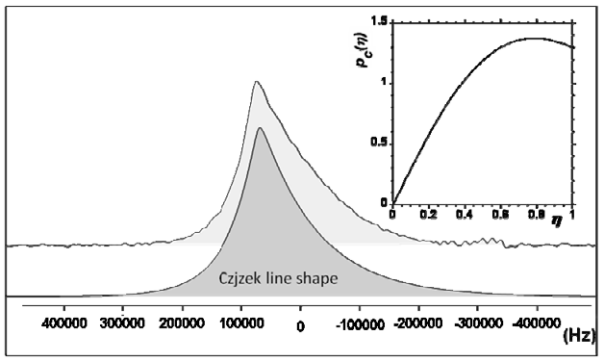

Figure 18. An experimental ^{71}Ga spectrum in a fluoride ionic glass from the pseudo-ternary system PbF_2–ZnF_2–GaF_3 whose shape is very well accounted for by a Czjzek line and the Czjzek distribution of η (shown in the inset).

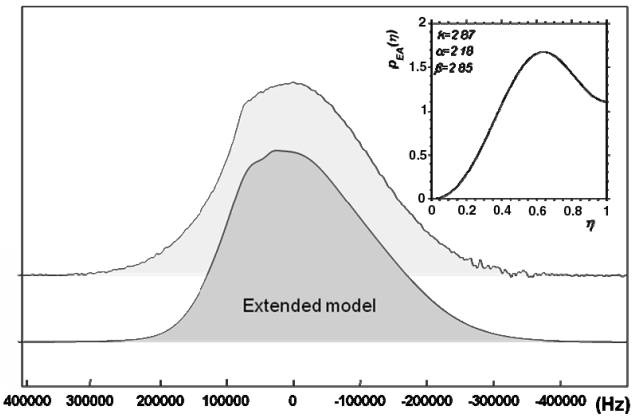

Figure 19. An experimental ^{71}Ga spectrum in a chalcogenide covalent glass, 25% GeS_2 + 75%Ga_2S_3, whose shape is very well accounted for by the extension of the Czjzek model for $\eta_0 = 0.6$, $\varepsilon = 0.3$, $\nu_Q = 6400$ kHz, FWHM = 1920 kHz and the associated distribution of η ($k = 2.87, \alpha = 2.18, \beta = 2.85$) shown in the inset.

to account fairly well for the observed shape (figure 19) with $\eta_0 = 0.6$, $\nu_Q = 6400$ kHz and $\varepsilon = 0.3$ ($k = 2.87, \alpha = 2.10, \beta = 2.85$). The spectrum was calculated with the dmfit software [54], which has been upgraded to include the extended Czjzek model in static mode. Further, it is worth comparing the lineshape associated with the standard Czjzek model to that of the extended model. The distribution of the asymmetry parameter η_Q of the Czjzek model is rather smooth, with a regular increase when η_Q increases from 0 to ∼0.8, followed by a small decrease for η_Q larger than ∼0.8 (figure 18), whereas those of the extended model are clearly peaked on a given value for values of ε which are not too large, for instance 0.6 (figure 19). The good agreement between the reconstructed line and the experimental one is in line with the fact that the chemical bond between gallium and its first neighbours is covalent. Since gallium is only four-fold coordinated, via directional covalent bonds, it seems reasonable to assume that some kind of local order is retained in the glass which imposes rather well-defined local values of $\eta_0 = \eta_{Q0} = 0.6$ and $\nu_Q(0) \approx 6200$ kHz. Nevertheless, it is a disordered network, as reflected by the quite large value of the ratio $\Gamma_{\eta_0}(\approx\varepsilon = 0.3)$ (equation (21)) needed to account for the broad smooth NMR line.

Finally, it is worth following the evolution of the shape of the quadrupolar lines when $\Gamma_{\eta_0}(=\Gamma)$ increases for different values of η_0 (figure 20, $\nu_Q(0) = 5000$ kHz). As expected, the static lines exhibit, for small Γ values, the classical discontinuities which characterize the quadrupolar interaction in a crystalline environment. For large values of Γ, and for any η_0, the broad line corresponding to a Czjzek distribution of quadrupolar parameters is retrieved and the local order is fully hidden. In between, some new shapes of NMR quadrupolar lines appear which depend both on η_0 and on Γ. The η_0 value points to the existence of an inherent local symmetry around the quadrupolar nucleus, whereas the Γ (or ε) factors reveals the degree of disorder characterizing the more remote network.

A possible method to compare experimental spectra with those predicted by the extended model is first to determine

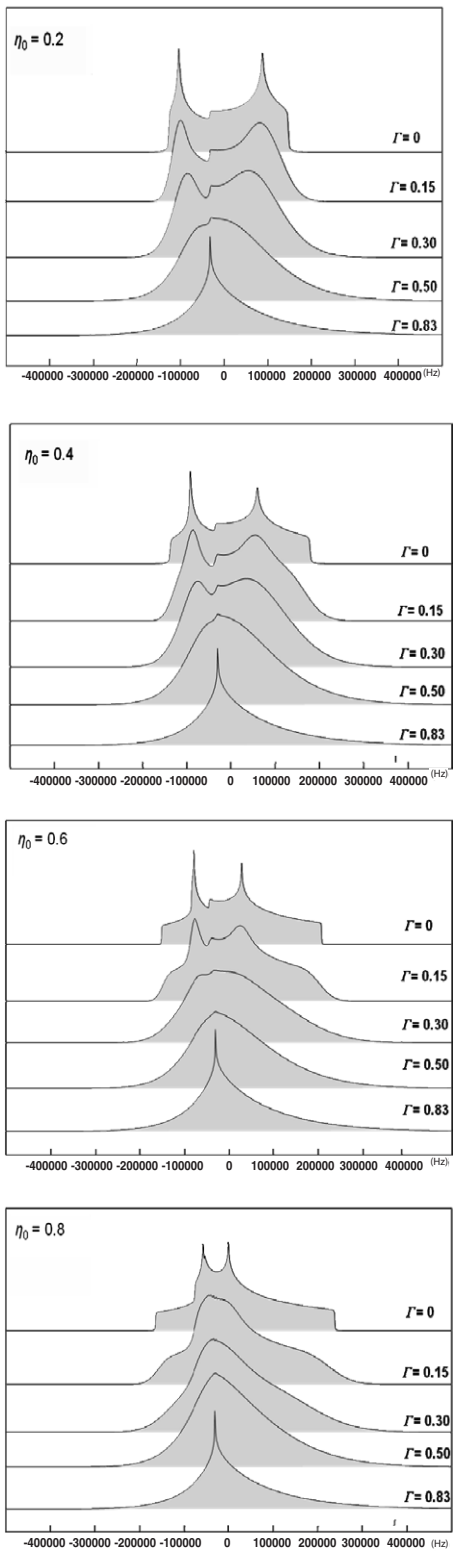

Figure 20. Calculated line shapes for ^{71}Ga for the extended Czjzek model for the indicated values of η_0 ($\nu_Q(0) = 5000$ kHz) and various values of the ratio $\Gamma = \Gamma_{\eta_0}(\varepsilon)$. For $\Gamma <\sim 0.5$, $\varepsilon \approx \Gamma$ (figure 3).

ε either from experimentally determined ratios, for instance from $r_{\eta_0}(\varepsilon)$ (figure 2 or equation (20)) or from $\Gamma_{\eta_0}(\varepsilon)$ (figure 3 or equation (21)). Then a value of η_0 is selected and a spectral shape consistent with the extended Czjzek model is calculated and compared to the experimental one. The asymmetry parameter η_0 is varied until an eventual agreement with experiment is found.

6. Conclusion

The Czjzek model represents a well-defined reference state for the distributions of the EFG tensor and of the EFG vector and consequently for the bivariate distribution of η and of V_{zz}. As discussed in the present paper, it is as uniform as it can be, without violating the constraints imposed by statistical isotropy, because of the applicability of a central limit theorem to the EFG vector. These two conditions are physically realistic for a wealth of disordered solids (ionic solids, alloys with long-range oscillatory interaction potentials, ...) and result in a tremendous simplification of the derivation of the EFG distribution, but at the cost of a loss of local structural information about the investigated solid. It is a perfect illustration of a behaviour commonly found in physics, as emphasized by the following passage of [55]: 'The statistical distribution of quantities that involves many microscopic variables is frequently independent of the assumptions made at the microscopic level and depends only upon very general macroscopic properties of the problem .... A central limit theorem is normally responsible for such a behaviour.'

A simple extension of the Czjzek model was investigated in detail. It is intended to mimic a well-defined local environment perturbed by disorder of more remote atoms whose effect is rendered by a Czjzek noise with an adjustable weight $\rho(\varepsilon)$ relative to the fixed $\bar{\boldsymbol{V}}(0)$. In that way, the number of free parameters is kept at a reasonable level, three, $V_{zz}(0)$, η_0, ε, as compared to a sole scale factor for the Czjzek model. Its characteristics are described as a function of η_0 and of ε with the aim to offer a practical tool which may help to retrieve, as far as possible, the information about the local environment provided by hyperfine techniques and notably by NMR. For small values of ε, the extended model exhibits situations in which the distribution of $|V_{zz}|$ and that of η are both Gaussians. Gaussian distributions of $\nu_Q \propto |V_{zz}|$ and of η are sometimes used, most often empirically, to reconstruct experimental NMR line shapes. That extension was shown to be helpful to describe some ^{71}Ga NMR spectra of covalent glasses. Its pertinence in a ^{17}O NMR theoretical and experimental study of sodium metaphosphate glasses will be described in a forthcoming paper [56].

The extended model might be considered as somewhat sketchy but it can provide useful information while being still simple. Knowing the variety of situations that can be encountered, an obvious and difficult question is: how to go farther? A way to make the present extended model more realistic would be to increase the number of free parameters, but with the risk of making it inapplicable and of leading to a situation in which the only solution left is to perform theoretical calculations from model structures. A first step might, however, be to distribute the elements of the 'fixed' EFG tensor on a sound physical basis.

Appendix

A different way of looking at the EFG tensor from two vectors in 3D space is worth describing. The method, recently applied to the study of the cosmic microwave background, involves multipoles with $2l+1$ degrees of freedom which are irreducible representations of the rotation group in 3D [19, 20]. As we consider the EFG tensor, we restrict the following to the multipole with $l = 2$ ($2l + 1 = 5$). Any real spherical function with fixed l is represented by a set of l 3D unit vectors $\boldsymbol{u}_1, \ldots, \boldsymbol{u}_l$ which is called a Maxwell multipole [20]. The elements of the EFG tensor can be constructed from these two vectors as [19]

$$v_{ij} = A\left(\frac{u_{1i}u_{2j} + u_{1j}u_{2i}}{2} - \frac{1}{3}\delta_{ij}\vec{u}_1 \cdot \vec{u}_2\right) \quad (i, j = x, y, z) \tag{A.1}$$

where A is a scale factor. The eigenvectors and the eigenvalues are then explicit expressions of $\boldsymbol{u}_1, \boldsymbol{u}_2$ and $X = \boldsymbol{u}_1 \cdot \boldsymbol{u}_2$. The three eigenvalues are for instance given by $A(X + 3)/6$, $A(X - 3)/6$ and $-AX/3$ [19] so that $\Delta = |V_{zz}|\sqrt{1 + \eta^2/3} = A\sqrt{(3 + X^2)}/3$. For a statistically isotropic solid, the vectors $\boldsymbol{u}_1$ and $\boldsymbol{u}_2$ play similar roles. Fixing their origins at a given point, the tip of each vector is uniformly distributed on the surface of a 3D unit sphere, but they are correlated. The sole knowledge of the distribution of X, $q(X)(-1 \leqslant X \leqslant 1)$ allows us to derive the distribution $p(\eta)$ as $|X| = \frac{3(1-\eta)}{(3+\eta)}$. Indeed, defining $q^+(X) = q(X)+q(-X)(0 \leqslant X \leqslant 1)$, yields

$$p(\eta) = \frac{12}{(3 + \eta)^2} q^+\left(\frac{3(1 - \eta)}{(3 + \eta)}\right) \qquad (0 \leqslant \eta \leqslant 1). \tag{A.2}$$

The distribution $q^+(Y)$ of $Y = |X|$ is reciprocally calculated from the distribution $p(\eta)$ (equation (A.2)) by replacing $p(\ )$ by $q^+(\ )$ and conversely by replacing η by Y. The distribution

$$q_{gi}(X) = \frac{27(1 - X^2)}{2(3 + X^2)^{5/2}} \tag{A.3}$$

is derived for a statistically isotropic spherical function which is a linear combination of the five spherical harmonics $Y_2^m(\theta, \varphi)$ $(m = -2, \ldots, 2)$ with independent identically distributed Gaussian coefficients (equation (9) of [19] and (11) of [20]). Then the Czjek distribution $p_C(\eta)$ is recovered from $q_{gi}^+(X) = 2q_{gi}(X)$ by applying equation (A.2). These results are independent of the value of the scaling A (equation (A.1)), which may be either fixed or distributed according to some law. Possible expressions of $\boldsymbol{u}_1$ and $\boldsymbol{u}_2$, which are useful for Monte Carlo simulations, are for a given $X = \boldsymbol{u}_1 \cdot \boldsymbol{u}_2$:

$$\boldsymbol{u}_1 \begin{cases} \sin\theta_1 \cos\varphi_1 \\ \sin\theta_1 \sin\varphi_1 \\ \cos\theta_1 \end{cases} \qquad \boldsymbol{u}_2 = X\boldsymbol{u}_1 + Z\boldsymbol{u}_{1\perp}$$

$$\boldsymbol{u}_{1\perp} = \begin{cases} -\sin\varphi_1 \sin\varphi_2 + \cos\theta_1 \cos\varphi_1 \cos\varphi_2 \\ \cos\varphi_1 \sin\varphi_2 + \cos\theta_1 \sin\varphi_1 \cos\varphi_2 \\ -\sin\theta_1 \cos\varphi_2 \end{cases} \tag{A.4}$$

with $0 \leqslant \theta_1 \leqslant \pi, 0 \leqslant \varphi_1, \varphi_2 \leqslant 2\pi$ and $Z = \sqrt{1 - X^2}$. For a statistically isotropic solid and three independent uniform random variables $\omega_0, \omega_1, \omega_2$ on (0, 1), we obtain

$$\cos\theta_1 = 2\omega_0 - 1, \qquad \varphi_k = 2\pi\omega_k, \qquad k = 1, 2. \tag{A.5}$$

It suffices then to select X and A according to two given distributions $q(X)$ and $p(A)$ (or equivalently according to distributions $p(\eta)$ and $p(\Delta)$) to obtain in that way the distribution of the associated EFG vector and that of the EFG tensor.

References

[1] Czjzek G, Fink J, Götz F, Schmidt H and Coey J M D 1981 *Phys. Rev.* B **23** 2513–30
[2] Stöckmann H 1981 *J. Magn. Reson.* **44** 145–58
[3] d'Espinose de Lacaillerie J B, Fretigny C and Massiot D 2008 *J. Magn. Reson.* **192** 244–51
[4] Le Caër G, Dubois J M and Brand R A 1984 *Amorphous Metals and Non-Equilibrium Processing* ed M von Allmen (Les Ulis: Editions de Physique) pp 249–54
[5] Le Caër G, Brand R A and Dehghan K 1985 *J. Physique Coll.* **46** C8 169–73
[6] Le Caër G and Dubois J M 1987 *Key Eng. Mater.* **13–15** 555–66
[7] Le Caër G and Brand R A 1998 *J. Phys.: Condens. Matter* **10** 10715–74
[8] Feller W 1957 *An Introduction to Probability Theory and its Applications* vols 1 and 2 (New York: Wiley)
[9] Czjzek G 1982 *Nucl. Instrum. Methods* **199** 37–44
[10] Egami T, Dmowski W, Kosmetatos P, Boord M, Tomida T, Oikawa E and Inoue A 1995 *J. Non-Cryst. Solids* **192/193** 591–4
[11] Tomida T and Egami T 1991 *J. Appl. Phys.* **69** 5451–3
[12] Rountree C L, Vandembroucq D, Talamali M, Bouchaud E and Roux S 2009 *Phys. Rev. Lett.* **102** 195501
[13] Srolovitz D, Maeda K, Takeuchi S, Egami T and Vitek V 1981 *J. Phys. F: Met. Phys.* **11** 2209–19
[14] Egami T 2006 *Intermetallics* **14** 882–7
[15] Bieri J B, Sanchez J, Fert A, Bertrand D and Fert A R 1982 *J. Appl. Phys.* **53** 2347–9
[16] Jaynes E T 1989 *ET Jaynes: Papers on Probability, Statistics and Statistical Physics* ed R D Rosenkrantz (Dordrecht: Kluwer) chapter 10
[17] Johnson O and Suhov Y 2001 *J. Stat. Phys.* **104** 145–65
[18] Devroye L 1986 *Non-Uniform Random Variate Generation* (New York: Springer)
[19] Land K and Magueijo J 2005 *Mon. Not. R. Astron. Soc.* **362** L16–9
[20] Dennis M R 2005 *J. Phys. A: Math. Gen.* **38** 1653–8
[21] Czjzek G 1982 *Phys. Rev.* B **25** 4908–10
[22] Legein C, Buzare J Y, Emery J and Jacoboni C 1995 *J. Phys.: Condens. Matter* **7** 3853–62
[23] Legein C, Buzaré J Y, Boulard B and Jacoboni C 1995 *J. Phys.: Condens. Matter* **7** 4829–46
[24] Legein C, Buzaré J Y and Jacoboni C 1996 *J. Phys.: Condens. Matter* **8** 4339–50
[25] Scholz G, Stösser R, Klein J, Silly G, Buzaré J Y, Laligant Y and Ziemer B 1996 *J. Phys.: Condens. Matter* **14** 2101–17
[26] Massobrio C, Celino M, Salmon P S, Martin R A, Micoulaut M and Pasquarello A 2009 *Phys. Rev.* B **79** 174201
[27] Johnson N L and Kotz S 1995 *Continuous Univariate Distributions* 2nd edn, vol 2 (New York: Wiley)
[28] Dumitriu I and Edelman A 2005 *Ann. Inst. Henri Poincaré* B **41** 1083–99

[29] Stacy E W 1962 *Ann. Math. Stat.* **33** 1187–92
[30] Massiot D, Kahn-Harari A, Michel D, Muller D and Taulelle F 1990 *Magn. Reson. Chem.* **28** S82–8
[31] Bureau B, Silly G, Buzaré J Y, Boulard B and Legein C 2000 *J. Phys.: Condens. Matter* **12** 5775–88
[32] Jeanneau E, Audebrand N, Le Floch M, Bureau B and Louer D 2003 *Solid State Chem.* **170** 330–8
[33] Neuville D R, Cormier L and Massiot D 2004 *Geochim. Cosmochim. Acta* **68** 5071–9
[34] Arean C O, Delgado M R, Montouillout V and Massiot D 2005 *Z. Anorg. Allg. Chem.* **631** 2121–6
[35] Seneschal K, Smektala F, Bureau B, Le Floch M, Jiang S, Luo T, Lucas J and Peyghambarian N 2005 *Mater. Res. Bull.* **40** 1433–42
[36] Presciutti F, Capitani D, Sgamellotti A, Brunetti B G, Costantino F, Viel S and Segre A 2005 *J. Phys. Chem.* B **109** 22147–58
[37] Neuville D R, Cormier L and Massiot D 2006 *Chem. Geol.* **229** 173–85
[38] Quintas A, Charpentier T, Majérus O, Caurant D, Dussossoy J L and Vermaut P 2007 *Appl. Magn. Reson.* **32** 613–34
[39] Angeli F, Gaillard M, Jollivet P and Charpentier T 2007 *Chem. Phys. Lett.* **440** 324–8
[40] Keppert M, Rakhmatullin A, Simko F, Deschamps M, Haarberga G M and Bessada C 2008 *Magn. Reson. Chem.* **46** 803–10
[41] Hoatson G L, Zhou D H H, Fayon F, Massiot D and Vold R L 2002 *Phys. Rev.* B **66** 224103
[42] Yahiaoui E M, Berger R, Servant Y, Kliava J, Čugunov L and Mednis A 1994 *J. Phys.: Condens. Matter* **6** 9415–28
[43] Bureau B, Silly G, Buzaré J Y, Legein C and Massiot D 1999 *Solid State Nucl. Magn. Reson.* **15** 129–38
[44] Bureau B, Guérault H, Silly G, Buzaré J Y and Grenèche J M 1999 *J. Phys.: Condens. Matter* **11** L423–31
[45] Brouwer W J, Davis M C and Mueller K T 2009 *Comput. Phys. Commun.* **180** 1973–82
[46] Bureau B, Troles J, Le Floch M, Guénot P, Smektala F and Lucas J 2003 *J. Non-Cryst. Solids* **319** 145–53
[47] Bureau B, Troles J, Le Floch M, Smektala F, Silly G and Lucas J 2003 *Solid State Sci.* **5** 219–24
[48] Bureau B, Troles J, Le Floch M, Guénot P, Smektala F and Lucas J 2003 *J. Non-Cryst. Solids* **326** 58–63
[49] Bureau B, Boussard-Plédel C, Troles J, Le Floch M, Smektala F and Lucas J 2005 *J. Phys. Chem.* B **109** 6130–5
[50] Zhang X H, Bureau B, Boussard-Plédel C, Ma H L and Lucas J 2008 *Chemistry* **14** 432–42
[51] Bureau B, Danto S, Ma H L, Boussard-Plédel C, Zhang X H and Lucas J 2008 *Solid State Sci.* **10** 427–33
[52] Ma H L, Calvez L, Bureau B, Le Floch M, Zhang X H and Lucas J 2007 *J. Phys. Chem. Solids* **68** 968–71
[53] Ledemi Y, Calvez L, Roze M, Zhang X H, Bureau B, Poulain M and Messaddeq Y 2007 *J. Optoelectron. Adv. Mater.* **9** 3751–5
[54] Massiot D, Fayon F, Capron M, King I, Le Calve S, Alonso B, Durand J O, Bujoli B, Gan Z H and Hoatson G 2002 *Magn. Reson. Chem.* **40** 70–6
[55] Mello PA 1986 *Quantum Chaos and Statistical Nuclear Physics* (*Lecture Notes in Physics*) vol 263 (Berlin: Springer) pp 267–84
[56] Vasconcelos F, Delevoye L, Cristol S, Paul J F and Le Caër G, in preparation